Dark mesons at the LHC

Graham D. Kribs,[a] **Adam Martin,**[b] **Bryan Ostdiek**[a] **and Tom Tong**[a]

[a]*Department of Physics, University of Oregon,*
Eugene, OR 97403 U.S.A.

[b]*Department of Physics, University of Notre Dame,*
South Bend, IN 46556 U.S.A.

E-mail: kribs@uoregon.edu, amarti41@nd.edu, bostdiek@uoregon.edu,
ttong2@uoregon.edu

ABSTRACT: A new, strongly-coupled "dark" sector could be accessible to LHC searches now. These dark sectors consist of composites formed from constituents that are charged under the electroweak group and interact with the Higgs, but are neutral under Standard Model color. In these scenarios, the most promising target is the dark meson sector, consisting of dark vector-mesons as well as dark pions. In this paper we study dark meson production and decay at the LHC in theories that preserve a global SU(2) dark flavor symmetry. Dark pions — like the pions of QCD — can be pair-produced through resonant dark vector meson production, $pp \to \rho_D \to \pi_D \pi_D$, and decay in one of two distinct ways: "gaugephobic", when $\pi_D \to f\bar{f}'$ generally dominates; or "gaugephilic", when $\pi_D \to W + h$, $Z + h$ dominates once kinematically open. Unlike QCD, the decay $\pi_D^0 \to \gamma\gamma$ is virtually absent due to the dark flavor symmetry. We recast a vast set of existing LHC searches to determine the current constraints on (and future opportunities for) dark meson production and decay. When m_{ρ_D} is slightly heavier than $2m_{\pi_D}$ and $\rho_D^{\pm,0}$ kinetically mixes with the weak gauge bosons, the 8 TeV same-sign lepton search strategy sets the best bound, $m_{\pi_D} > 500\,\text{GeV}$. Yet, when only the ρ_D^0 kinetically mixes with hypercharge, we find the strongest LHC bound is $m_{\pi_D} > 130\,\text{GeV}$, that is only slightly better than what LEP II achieved two decades ago. We find the relative insensitivity of LHC searches, especially at 13 TeV, can be blamed mainly on their penchant for high mass objects or large missing energy. Dedicated searches would undoubtedly yield substantially improved sensitivity. We provide a GitHub page to speed the implementation of these searches in future LHC analyses. Our findings for dark meson production and decay provide a strong motivation for *model-independent* searches of the form $pp \to A \to B + C \to \text{SM SM} + \text{SM SM}$ where the theoretical prejudice is for SM to be a 3rd generation quark or lepton, W, Z, or h.

https://doi.org/10.1007/JHEP07(2019)133

Contents

1 Introduction

We consider extensions of the Standard Model that incorporate a new, strongly-coupled, confining gauge theory with fermion representations that transform under the electroweak group. There are a wide variety of uses of a new, strongly-coupled, confining group. One use is to at least partially break electroweak symmetry dynamically, such as bosonic technicolor [1–9] and the closely related ideas on strongly-coupled induced electroweak symmetry breaking [10–20]. Composite Higgs theories also posit a new strongly-coupled sector in which at least an entire Higgs doublet emerges in the low energy effective theory (the literature is far too vast to survey, for a review see e.g., [21]). There is also a interesting connection to the relaxation of the electroweak scale [22] using a new strongly-coupled sector, e.g., [19, 20, 22–24].

Dark matter can emerge as a composite meson or baryon of a strongly-coupled theory, often with an automatic accidental symmetry that protects against its decay. Since the early days of technicolor there was a possibility of dark matter emerging as techni-baryons [25–31]. There is now a growing literature that has studied strongly-coupled dark matter as dark pions [32–53], dark quarkonia-like states [54–58], as well as dark baryons and related candidates [32, 36, 41, 55, 59–86] (for a review, see [87]).

Another use is to simply characterize generic strongly-coupled-like signals as targets for LHC and future colliders. Vector-like confinement [88] pioneered this study in the

context of vector-like fermions that transform under part of the SM group as well as under a new, strongly-coupled group with scales near or above the electroweak scale. Further explorations into the phenomenology and especially the meson sector included [20, 38, 55, 73, 89–97]. In theories with somewhat lower confinement scales, the dark sector may lead to dark showers and related phenomena [98–104], displaced signals [105, 106] and potentially intriguing spectroscopy [47, 107, 108]. Spectacular "quirky" signals can arise in theories with a very low confinement scale [109, 110]. The latter theories may also lead to a high multiplicity of soft particles that are tricky to observe [111–113].

In a companion paper [114], we develop dark sectors whose (ultraviolet) strongly-coupled sector preserves a SU(2) dark flavor symmetry. These theories are mapped into a low energy effective theory that provides the leading interactions of the dark mesons with the Standard Model. A dark sector that is of particular interest to us is Stealth Dark Matter [75]. In this theory, there is a new, strongly-coupled dark sector that consists of vector-like fermions that transform under both the new dark group as well as the electroweak part of the SM, and crucially, also permit Higgs interactions (from Yukawa couplings or higher dimensional operators). Others have also pursued dark sectors with vector-like fermions that permit Higgs interactions for a variety of purposes [20, 23, 43, 85, 115].

The dark meson sector of the Stealth Dark Matter theory has several intriguing properties due to the accidental symmetries of the model. Like vector-like confinement [88] the dark sector is free of constraints from precision electroweak observables and Higgs coupling measurements so long as the vector-like mass is dominant. Unlike vector-like confinement, however, the Higgs interactions break the global (species) symmetries of the dark sector, permitting dark pions to decay into SM states. Provided the vector-like masses are smaller than $\sim 4\pi f$, where f is the scale of the new strong interaction, we can organize the states using chiral perturbation theory. In this paper we focus on the most phenomenologically relevant states: the (lightest) triplet of pseudoscalar pions π_D^a and the heavier triplet of vector mesons ρ_D^a [116, 117]. The scales of the theory, as we will see, are comparable to or somewhat larger than the electroweak scale.

The presence of a SU(2) dark flavor symmetry arises from global symmetries of the ultraviolet strongly-coupled sector. For example, a strongly-coupled sector that contains two flavors of dark fermions with identical (current) masses has a global SU(2) × SU(2) symmetry that is broken by the condensate to a SU(2) dark flavor symmetry [114]. This is just like QCD with its two light flavors of quarks with nearly equal (current) masses. In ref. [114], we demonstrate strongly-coupled theories where the SU(2) dark flavor symmetry can be identified as an exact custodial symmetry of the dark sector. That is, the Higgs multiplet interacts with the dark flavors such that the SO(3) $\sim$ SU(2)$_c$ is not further broken by the dark sector. Consequently, the dark sector's meson degrees of freedom can be categorized in custodial symmetric representations. Again considering the example of theories with two flavors of dark fermions, the meson sector contains dark pions and one set of dark vector mesons in a triplet representation of the SU(2) dark flavor symmetry. Unlike QCD, however, the vector-like nature of the dark sector permits two possibilities for gauging the global flavor symmetry: the entire SU(2) could be gauged (the SU(2)$_L$ weak

interaction) or just the U(1) (as in U(1)$_B$ hypercharge).[1] This leads to two distinct low energy effective theories of dark mesons:

$$
\begin{aligned}
\mathrm{SU(2)}_L \ \ \text{model}: \quad \mathrm{SU(2)}_{\text{global flavor}} &\leftrightarrow \mathrm{SU(2)}_L \\
\mathrm{SU(2)}_R \ \ \text{model}: \quad \mathrm{SU(2)}_{\text{global flavor}} &\leftrightarrow \mathrm{SU(2)}_R
\end{aligned}
\tag{1.1}
$$

In the latter case, obviously only the U(1) subgroup is gauged, but since we assume the dark sector respects the full global SU(2), we'll refer to this as the SU(2)$_R$ model.

In the meson sector the dark pion states can be pair-produced, either via Drell-Yan or resonantly via mixing of the ρ with SM electroweak gauge bosons. Several groups have studied pair production of weakly coupled states including [73, 88, 89, 118–120]. The dark pion decays can be categorized into two distinct possibilities: "gaugephobic", when $\pi_D \to f\bar{f}'$ dominates; or "gaugephilic", when $\pi \to W + h$, $Z + h$ dominates once kinematically open. The decay $\pi_D^0 \to \gamma\gamma$ is highly suppressed due to the dark flavor symmetry [114]. For a wide range of parameters, the interaction between single dark pions and the SM is small enough to make single pion production phenomenologically irrelevant, and yet, the interaction can be easily large enough that the dark pions decay *promptly* back to SM states. We also briefly comment on the possibility that dark pions are sufficiently long-lived so as to modify their phenomenological signature.

Dark mesons are therefore an example of new physics that must be pair produced with $\sim$ weak strength and decay back to multiple SM particles (only). The combination of a relatively low production cross section and complex final states with no BSM sources of missing energy leads to weak LHC constraints. We perform a detailed breakdown of which LHC searches could potentially set bounds on dark mesons. For the searches with potential, we recast the searches and estimate the bounds for some benchmark dark meson scenarios. For the searches that fail, we identify why. This latter step is useful as we find many 13 TeV analysis are insensitive to dark mesons because their cut thresholds are too high.

The layout of the rest of this paper is as follows. In section 2 we introduce our phenomenological dark meson model and its relevant parameters. This model description is broken up into three parts: the strong sector, kinetic mixing, and π_D decay. Using this setup, we explore the constraints on dark meson parameter space. Section 3 is devoted to constraints from single ρ_D production, while we explore constraints from π_D pair production in section 4. We step through the details of the searches that provide constraints and provide insight into why other searches fail to. Finally, we present our conclusions in section 5.

2 Phenomenological description of dark mesons

The dark meson interactions will be described below using a phenomenological lagrangian. The core philosophy was formulated in "vector-like confinement" [88, 89], and our discussion

---

[1]It is also possible that there is some mixture between SU(2)$_L$ and SU(2)$_R$, but this requires more than just a single triplet of dark pions and dark vector mesons. More details can be found in ref. [114].

of resonant production of dark pions through a dark rho parallels theirs. The key distinction between our formulation and vector-like confinement is the presence of Higgs interactions among the dark fermions which breaks enough of the dark flavor symmetries to allow dark pions to decay. In the language of vector-like confinement, all species symmetries are broken by Higgs interactions in the dark sector (either Yukawa couplings or higher-dimensional interactions).

2.1 Dark mesons in SU(2) triplet representations

The lagrangian can be written as

$$\mathcal{L} = \mathcal{L}_{\text{strong}} + \mathcal{L}_{\text{kinetic mixing}} + \mathcal{L}_{\text{decay}} \,. \tag{2.1}$$

The first contribution contains the meson sector of the theory as it arises from the strongly-coupled dark sector:

$$\mathcal{L}_{\text{strong}} = -\frac{1}{4}\rho_{D\,\mu\nu}^{a}\rho_D^{a\mu\nu} - \frac{m_{\rho_D}^2}{2}\rho_{D\,\mu}^{a}\rho_D^{a\mu} \tag{2.2}$$

$$+ \frac{1}{2}\left(D_\mu\pi_D^{a}\right)^\dagger\left(D^\mu\pi_D^{a}\right) - \frac{1}{2}m_{\pi_D}^2\pi_D^{a}\pi_D^{a} \tag{2.3}$$

$$- g_{\rho_D\pi_D\pi_D}f^{abc}\rho_{D\,\mu}^{a}\pi_D^{b}D^\mu\pi_D^{c}, \tag{2.4}$$

It contains the kinetic terms of the vector (ρ_D) and pseudoscalar (π_D) mesons, mass terms, and the interactions among these mesons. As we indicated in the introduction, the mesons fill out representations of the SU(2) dark flavor symmetry, and the meson self-interactions respect the SU(2) dark flavor symmetry. Throughout all of these expressions, we have assumed that the dark sector contains (at least) one set of dark pions and (at least) one set of dark vector mesons in the triplet representation of the SU(2) dark flavor symmetry. Hence the $a = 1, 2, 3$ index attached to π_D^a and ρ_D^a.[2] We will only consider the phenomenological consequences of the lightest triplet dark vector meson (ρ_D^a) and the lightest triplet dark pion (π_D^a).

The coupling between the ρ_D and π_D is show in eq. (2.4). This is the analogue of $g_{\rho\pi\pi}$ in QCD. In the SU(2)$_R$ model, the full set of SU(2)$_R$-symmetric interactions are present, though in practice only the $\rho_D^0\pi_D^+\pi_D^-$ interaction is phenomenologically relevant since only ρ_D^0 talks to SM fermions via kinetic mixing (see section 2.2). The NDA estimate of the coupling strength is given by

$$g_{\rho_D\pi_D\pi_D} \approx \frac{4\pi}{\sqrt{N_D}}. \tag{2.5}$$

2.2 Kinetic mixing of ρ_D with SM

The second term of eq. (2.1) contains the kinetic mixing of the dark rhos and the electroweak gauge bosons:

$$\mathcal{L}_{\text{kinetic mixing}} = -\frac{\epsilon}{2}\rho_{D\,\mu\nu}^{a}F^{a\mu\nu} = \begin{cases} -\frac{\epsilon}{2}\rho_{D\,\mu\nu}^{a}W^{a\mu\nu} & \text{SU(2)}_L \text{ model} \\ -\frac{\epsilon'}{2}\rho_{D\,\mu\nu}^{0}B^{\mu\nu} & \text{SU(2)}_R \text{ model} \end{cases} \tag{2.6}$$

---

[2]We use ρ_D^3 and ρ_D^0 interchangeably.

This provides the main "portal" from the Standard Model into the dark sector. There are two cases we detail below: $F^{a\mu\nu}$ identified with $W^{a\mu\nu}$ (the $SU(2)_L$ model), and $F^{a\mu\nu}$ identified with $\delta^{a0}B^{\mu\nu}$ (the $SU(2)_R$ model).

In each of the models defined by eq. (1.1), all or part of the SU(2) dark flavor symmetry is gauged. In $SU(2)_L$ model, the triplet of global SU(2) is identified as a triplet of the gauged electroweak $SU(2)_L$ group. In the $SU(2)_R$ model, the triplet of global SU(2) is identified as a triplet of the would-be gauged electroweak $SU(2)_R$ group, had the entire $SU(2)_R$ been gauged. Of course the entire $SU(2)_R$ is not gauged — just the $U(1)_B$ subgroup. After electroweak symmetry breaking, $SU(2)_L \times U(1)_B \to U(1)_{\rm em}$, the triplet of vector and pseudoscalar mesons of the $SU(2)_L$ and $SU(2)_R$ models have the same electric charges, $Q = (+1, 0, -1)$.

In both models, we use naive dimensional analysis (NDA) to estimate the size of the kinetic mixing:

$$\begin{aligned} \epsilon &\approx \frac{\sqrt{N_D}}{4\pi} g, \quad SU(2)_L \text{ model} \\ \epsilon' &\approx \frac{\sqrt{N_D}}{4\pi} g' \quad SU(2)_R \text{ model}, \end{aligned} \tag{2.7}$$

strictly valid for a large number of colors N_D of the confining dark gauge group. Diagonalizing the kinetic terms leads to a field redefinition of

$$\begin{aligned} W_\mu^a &\to W_\mu^a - \epsilon\, \rho_{D\mu}^a \quad SU(2)_L \text{ model} \\ B_\mu &\to B_\mu - \epsilon'\, \rho_{D\mu}^0 \quad SU(2)_R \text{ model}, \end{aligned} \tag{2.8}$$

at leading order in ϵ. This leads to a ρ_D interaction with the SM fermions with a coupling strength proportional to g^2 or g'^2,

$$\mathcal{L}_{\rho_D f \bar{f}} = \begin{cases} \epsilon\, g\, \bar{f}_i\, \bar{\sigma}^\mu t_{ij}^a\, \rho_{D\mu}^a\, f_j & SU(2)_L \text{ model} \\ \epsilon' Y_f\, g'\, \bar{f}\, \bar{\sigma}^\mu\, \rho_{D\mu}^0 f & SU(2)_R \text{ model}, \end{cases} \tag{2.9}$$

where $f_{i,j}$ are left-handed SM fermions in the $SU(2)_L$ model, while f are any SM fermions with hypercharge Y_f in the $SU(2)_R$ model.

The difference between the two models is mainly in the kinetic mixing. In the $SU(2)_L$ model, the entire triplet of ρ_D^a mixes with the triplet of W^a bosons. In the $SU(2)_R$ model, only the neutral component of the triplet, ρ_D^0, mixes with the hypercharge gauge boson. Additionally, the kinetic mixing ϵ has one power of the gauge coupling: g in the $SU(2)_L$ model; g' in the $SU(2)_R$ model. Here we emphasize that while the difference between $g/g' \simeq 2$ may seem small or trivial, $pp \to \rho$ production is proportional to $3g^4$ in the $SU(2)_L$ model (compared with g'^4 in the $SU(2)_R$ model), and so this leads to a significant difference in the production rates of ρ_D's in the two models.

Neglecting mass differences among states within the triplets, the strong sector is thus described by three parameters:

$$m_{\pi_D}, \ m_{\rho_D}, \ N_D \quad \text{or equivalently} \quad m_{\pi_D}, \ \eta \equiv \frac{m_{\pi_D}}{m_{\rho_D}}, \ N_D\,. \tag{2.10}$$
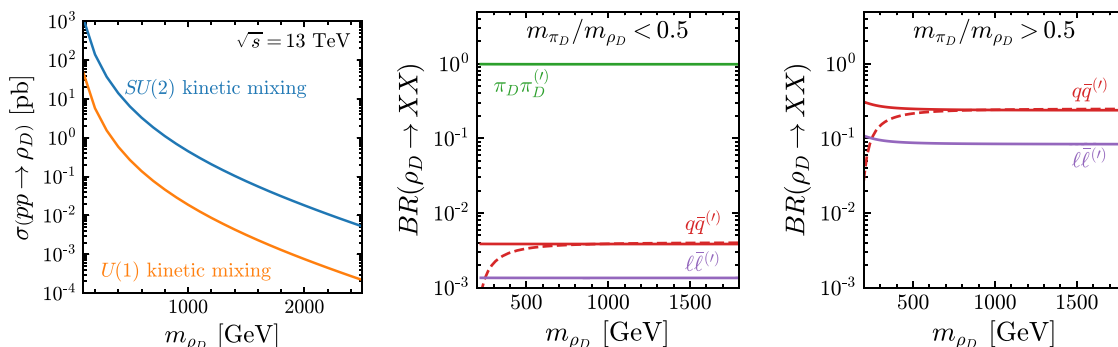
Figure 1. The left panel shows the production cross section at $\sqrt{s} = 13$ TeV for the dark vector mesons. The blue and orange lines depict whether the vector mesons are $SU(2)_L$ or $SU(2)_R$ symmetric and kinetically mix with the appropriate standard model gauge bosons. The middle and right panels show the subsequent branching ratio for the ρ_D depending on whether or not it can decay to the π_D. The red lines denote decays to quark anti-quark pairs, and the dashed line indicates the top quark. The purple lines show leptonic decays.

As our canonical example that we use throughout this paper, we have taken $N_D = 4$ in the bulk of our results below. This choice was motivated by the Stealth Dark Matter model [75]; the phenomenology is broadly similar so long as the number of colors is not excessive. We quantify this in detail below.

Additionally, we will often replace one of the dark meson mass parameters for the ratio $\eta = m_{\pi_D}/m_{\rho_D}$. This ratio is important because it governs how the ρ_D can decay. Specifically, if $\eta < 0.5$, ρ_D can decay to a pair of dark pions, while if $\eta > 0.5$ the dark rhos must decay directly back to SM particles. As we will see, the latter case is strongly constrained by limits from Z', W' searches. From now on, we will label our dark meson models by the type of kinetic mixing and the ratio of dark meson masses, i.e.,

$$\mathrm{SU}(2)_L^\eta: \qquad \epsilon = g\sqrt{N_D}/(4\pi), \qquad \epsilon' = 0$$

$$\mathrm{SU}(2)_R^\eta: \qquad \epsilon = 0, \qquad \epsilon' = g'\sqrt{N_D}/(4\pi)$$

Having specified N_D, the production cross section for ρ_D is completely determined for both models as shown in the left-side plot in figure 1. Figure 1 also shows the ρ_D branching ratios for two different η values: as expected, if $\eta < 0.5$ (middle panel) then the interaction strength and form of the $\rho_D \pi_D \pi_D$ interaction make $\rho_D \to \pi_D \pi_D$. On the other hand, if the π_D are too heavy ($\eta > 0.5$, right plot), the ρ_D decay back through kinetic mixing and the branching ratios are simply determined by the SM color factors.

In focusing on the two models, we are ignoring scenarios where the $\mathrm{SU}(2)_L \times \mathrm{U}(1)_Y$ properties of the ρ_D [and π_D] are not well defined. Generally, large mixing can only happen in scenarios where the strong sector plays a large role in electroweak breaking and therefore faces constraints from Higgs coupling measurements and precision electroweak tests. In terms of ρ_D phenomenology, having well defined $\mathrm{SU}(2)_L \times \mathrm{U}(1)_Y$ properties means that the $\rho_D \to V\pi_D$ ($V =$ SM electroweak boson) decay modes are always small.

We would be remiss to not point out that the $\mathrm{SU}(2)_R$ model invovling a dark $\mathrm{U}(1)$ vector boson mixing between the hypercharge is ubiquitious in the literature of simple dark

sectors as "dark photons" (e.g., for a review [121]). While most of this literature focuses on (much) lighter dark photons, for simple dark photon models with a dark photon mass at or above the electroweak scale, we can map this toy model onto a special case of our strongly-coupled dark sector. The mapping utilizes the $SU(2)_R$ model with: $\eta > 0.5$ (so that the dark vector boson can decay only into SM states), $m_{\rm SM}/v_\pi$ small (so that single production of dark pions is negligible), and the number of dark colors N_D chosen to obtain a kinetic mixing ϵ'. Even with these parameter choices, our strongly-coupled dark sector obviously has differences from the simple toy models. One is that the kinetic mixing is at most one-loop suppressed. Another is that there is relationship between the smallness of the kinetic mixing, the number of dark colors, and the relative size of self-interactions of the dark mesons. While it would be interesting to map out this space more fully, this is beyond the scope of this paper.

2.3 Dark pion decay to SM

Finally, dark pion decay. This is the main subject of our companion paper [114]. There we show that strongly-coupled models with custodially-symmetric Higgs interactions among the dark fermions leads to a low energy effective theory in which dark pions interact with the SM through:

$$
\begin{aligned}
\mathcal{L}_{\rm decay} = \frac{\sqrt{2}}{v_\pi} & \left[\pi_D{}^+ \bar{\psi}_u (m_d P_R - m_u P_L)\psi_d + \pi_D{}^- \bar{\psi}_d (m_d P_L - m_u P_R)\psi_u \right. \\
& \left. + \frac{i}{\sqrt{2}} \pi_D{}^0 (m_u \, \bar{\psi}_u \gamma_5 \psi_u - m_d \, \bar{\psi}_d \gamma_5 \psi_d) \right] \\
- \xi \frac{m_W}{v_\pi} & \left[(W_\mu^- h \overleftrightarrow{\partial}^\mu \pi_D{}^+) + (W_\mu^+ h \overleftrightarrow{\partial}^\mu \pi_D{}^-) + \frac{1}{\cos\theta_W}(Z_\mu h \overleftrightarrow{\partial}^\mu \pi_D{}^0) \right]
\end{aligned}
\tag{2.11}
$$

where $\psi_{u,d}$ are SM fermions. There are several important features of this Lagrangian. First, while we have used the language that the decay interactions 'break the flavor symmetry', this is slightly sloppy. Stated more correctly, we have married the $SU(2)_V$ symmetry of the dark pions to part of the $O(4)$ symmetry group of the Higgs potential. Both the dark pions and the SM fields transform under the shared symmetry, so we can write down single pion interactions of the form $\pi^a \mathcal{O}^a$ where $\mathcal{O}^a$ is some triplet of SM fields.

The overall scale of the operators is set by $1/v_\pi$ for the fermions and ξ/v_π for the gauge/Higgs bosons. The fact that the interactions do not further distinguish the fermions (i.e., one overall coupling for the first four terms) nor the gauge/Higgs interactions (one coupling for the last three terms) is due to the the dark sector's preservation of custodial symmetry. However, since custodial SU(2) is broken in the SM by differences of Yukawa couplings as well as hypercharge, there is a residual differentiation of the interactions by $m_u - m_d$ as well as $g' \neq 0$.

This form is convenient, since coupling π_D to the SM fields requires breaking electroweak symmetry and hence the coupling strengths must be proportional to the mass of a SM field. The primary role of the $1/v_\pi$ parameter is to set the total width of the π_D. In this paper our main focus is on scenarios where the π_D decay promptly. This sets a lower bound on m_{SM}/v_π, where m_{SM} is the mass of the mass of the SM particle(s) in

the dominant π_D decay. Scenarios where π_D is displaced or long-lived are also interesting to study. The main search methodologies are well-known from other displaced/long-lived searches (for a review, see e.g. [122]).

The remaining model-dependent parameter is the relative strength of the coupling to fermions versus the gauge/Higgs sector that we have parameterized by ξ. We will consider two possibilities for ξ:

$$\begin{aligned} \xi &= 1 && \text{``gaugephilic''} \\ \xi &= c_\xi \frac{v^2}{m_{\pi_D}^2} \ll 1 && \text{``gaugephobic''} \end{aligned} \tag{2.12}$$

The scaling of the gaugephobic parameter with the electroweak scale and the dark pion mass scale deserves some discussion. The origin of this scaling is found from an analysis of the strongly-coupled effective theories that we have discussed in detail in ref. [114]. In essence, there are higher dimensional operators involving additional Higgs fields, suppressed by at least the scale of the dark pions, that can regenerate couplings to the gauge/Higgs sector even if they don't exist at leading order. As we show in ref. [114], the Stealth Dark Matter model is gaugephobic with $\xi = m_h^2/(m_{K_D}^2 - m_h^2) \simeq m_h^2/m_{K_D}^2$ where K_D is a another dark pion that is at least slightly heavier than π_D. Since the dark kaon scales with the parameters of the ultraviolet theory in exactly the same way as the dark pion, in our phenomenological study we take $c_\xi = \lambda_h$ and do not distinguish between the dark pion and kaon masses.

In the limit that the dark pion mass scale is taken large, $\xi \to 0$, and the dark pions can only decay back to fermions. However, when the dark pions are near to the electroweak scale, ξ can be "smallish" but, importantly, nonzero. This implies $\pi_D \to f\bar{f}'$ dominate so long as there is no small coupling. For the specific case of π_D^0 in the mass range $m_h + m_Z < m_{\pi_D^0} < 2m_t$, the decay $\pi_D^0 \to Z + h$ dominates despite being gaugephobic. This is because the Zh mode is longitudinally enhanced, while the competing fermionic mode $\pi_D^0 \to b\bar{b}$ is suppressed by the small Yukawa coupling y_b. For all other ranges of dark pion masses (both charged and neutral), $\pi_D \to f\bar{f}'$ dominates. By contrast, in the gaugephilic case $\pi_D \to W + h$, $Z + h$ dominate once they are kinematically open.

While the two choices in eq. (2.12) may seem arbitrary at first, a large class of strongly-coupled models can be mapped into this categorization (see ref. [114] for more details). Specifically, the Stealth Dark Matter model [75, 76, 87] and others similar to it are gaugephobic. By contrast, models of bosonic technicolor / induced symmetry breaking [14], as well as the triplet state in Georgi-Machacek models [123] have gaugephilic interactions.

In our taxonomy, the gaugephilic case only occurs for the $\mathrm{SU}(2)_L$ model. This is not immediately obvious from our discussion thus far. Essentially the gauge/Higgs interactions on the last line of eq. (2.11) is permitted with order one ξ when π_D^a is in the same representation as W_μ^a, i.e., an $\mathrm{SU}(2)_L$ triplet. The reader may then immediately wonder why the $\mathrm{SU}(2)_R$ case does not have $\xi = 0$. At leading order it does, but at higher orders one finds gauge/Higgs interactions are generated albeit with a suppression typically of order $m_h^2/m_{\pi_D}^2$. This is parametrically the suppression we find in the Stealth Dark Matter model [114], and is similar to what we find in generic 2-flavor custodially-symmetric models. More details can be found in ref. [114].
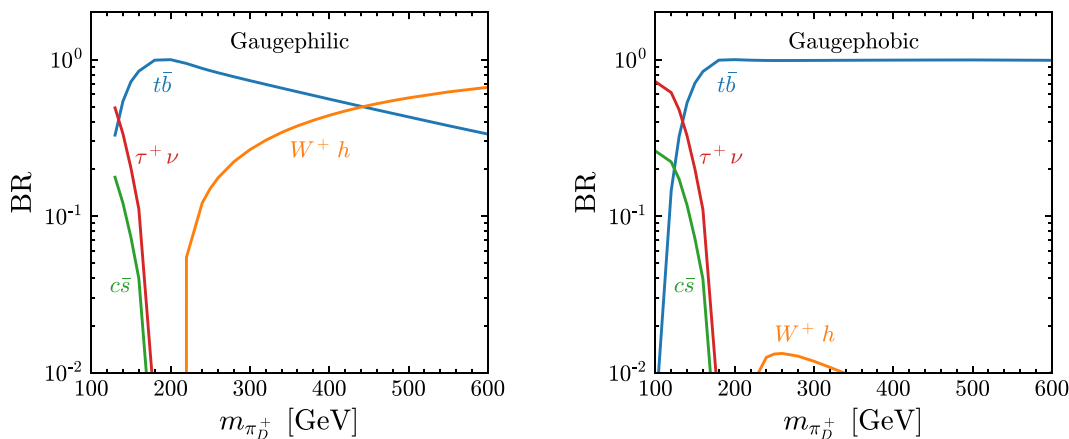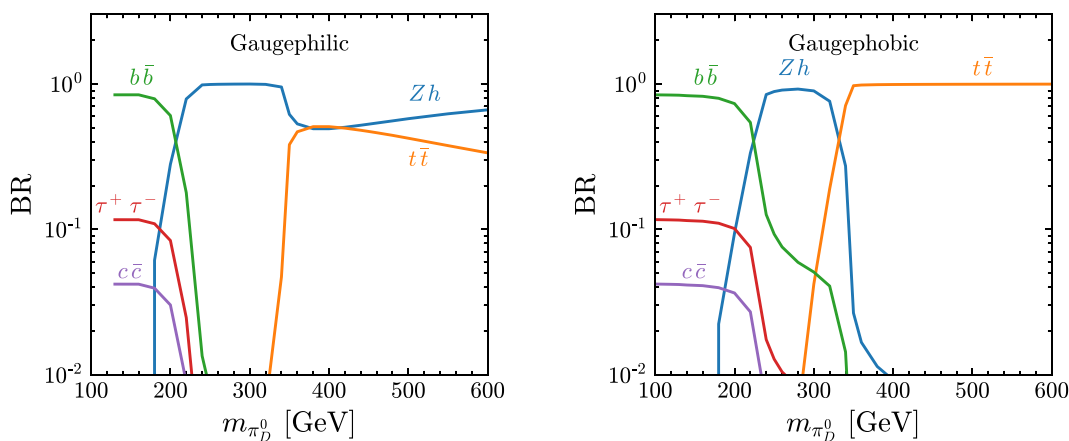
Figure 2. Branching ratios of the charged pions.

Figure 3. Branching ratios of the neutral pions.

Any given model may or may not permit arbitrary choices for v_π and ξ; for instance, induced electroweak symmetry breaking requires v_π fixed (up to order one coefficients) and $\xi = 1$ due to the requirements of proper electroweak symmetry breaking. However, as we detail in [114], there are models that span a wide range of $(v_\pi, \xi \lesssim 1)$.

Given ξ, the branching fractions of the π_D are fully specified as a function of the pion mass. As π_D decay couplings are proportional to mass, they decay to the heaviest kinematically available SM particles. The branching ratios for the gaugephilic and gaugephobic scenarios are compared side by side in figure 2 (charged π_D) and 3 (neutral π_D).[3]

For the charged π_D, the branching ratios in the two cases are similar at small masses. However, the unsuppressed gauge/Higgs couplings in the gaugephilic scenario imply $\pi_D \to W^+ h$ quickly dominates once it is kinematically allowed (due to the kinematic enhancement of decays to longitudinal W), while the $\pi_D \to t\bar{b}$ mode always dominates at heavy mass for

---

[3]We have omitted the anomaly-induced decay $\pi_D{}^0 \to \gamma\gamma$ from figure 3. In models with a SU(2) flavor symmetry that becomes custodial SU(2) after Higgs interactions, the dark sector is anomaly-free. The decay mode does reappear due to SM interactions violating custodial SU(2), but is highly suppressed so as to be phenomenologically irrelevant [114].

the gaugephobic case. There is a similar pattern in the branching ratio of the neutral pions. Again, when the pion is light, the decay modes between the two categories are similar and are dominated by the $b\bar{b}$ mode. This similarity persists after π_D passes the Zh threshold. However, as π_D is further increased past the $t\bar{t}$ threshold we can spot the difference, as the $\pi_D \to \bar{t}t$ branching ratio dominates at large π_D masses in the gaugephobic case but stays subdominant to Zh in the gaugephilic case.

3 Constraints from single production

Having established the dark meson phenomenological Lagrangian and fleshed out the relevant parameters, we now move on to LHC production, sensitivities, and constraints.

The phenomenology of the dark meson sector that we pursue in this paper clearly bifurcates at $\eta = 0.5$ as evident from the branching fractions of the dark pions in figure 1. For $\eta > 0.5$, the ρ_D is kinematically forbidden to decay to a pair of on-shell dark pions, and thus decays to SM fermions dominate.[4] The decays into SM fermions are determined solely by the gauge and color charges of the fermions, so the ρ_D phenomenology is essentially independent of the details of how the pions interact with the SM.

When $\eta < 0.5$, $\rho_D \to \pi_D \pi_D$ is open, and generally dominates so long as the number of dark colors, N_D, is not large (we'll be more precise below). In this case, the most promising way to search for dark mesons is dark pion pair production. The largest contribution to dark pion pair production is resonant production $pp \to \rho_D \to \pi_D \pi_D$ through the dark rho, so long as it is not very heavy. Dark pions can also be pair-produced through Drell-Yan production, though this tends to give a smaller cross section due to the W or Z exchange being off-shell. We find that resonant production through ρ_D dominates for $\eta \gtrsim 0.2$ for $N_D = 4$.

The final states populated by dark pion pairs depends on how the dark pions decay, which in turn depends on whether we are in a gaugephilic or gaugephobic scenario. We have chosen 9 benchmarks spanning the phenomenology possibilities that we believe give a solid idea of the differing phenomenology, shown in table 1. We provide the `FeynRules` [124] model files and corresponding UFO files on GitHub.[5]

We used `MadGraph5_aMC@NLO` [125] to simulate the events. When studying constraints directly on the ρ_D, we simulated $pp \to \rho_D$ and then allowed for any decay mode. For the constraints on π_D, we simulated $pp \to \pi_D \pi_D$ which then had resonant and Drell-Yan production. In all cases, showering and hadronization was performed by `Pythia 8` [126] and `Delphes 3` [127] was used for fast detector simulation. We used the default detector card because we recast both ATLAS and CMS results. Within `Delphes`, jets were calculated with `FastJet` [128] using the anti-k_t algorithm [129]

For each of the benchmark scenarios in table 1, the mass of the π_D was scanned with variable spacing in order to capture the different decay mode transitions. We take the lower limit of dark pion mass to be $100\,\mathrm{GeV}$, coming from the bound on BSM charged

---

[4]Figure 1 includes three-body decays though an off-shell dark pion, but the rates for these decay modes are always small compared to what is shown in the figure.

[5]https://github.com/bostdiek/HeavyDarkMesons

– 10 –

Model	$\eta \equiv m_{\pi_D}/m_{\rho_D}$	ξ
$SU(2)_L^{55}$	0.55	
$SU(2)_L^{45}$	0.45	gaugephilic ($\xi = 1$)
$SU(2)_L^{25}$	0.25	
$SU(2)_L^{55}$	0.55	
$SU(2)_L^{45}$	0.45	gaugephobic ($\xi = m_h^2/m_{\pi_D}^2$)
$SU(2)_L^{25}$	0.25	
$SU(2)_R^{55}$	0.55	
$SU(2)_R^{45}$	0.45	gaugephobic ($\xi = m_h^2/m_{\pi_D}^2$)
$SU(2)_R^{25}$	0.25	

Table 1. Benchmark models and parameters used in our study. Note that the gaugephilic case only occurs for the $SU(2)_L$ model, as discussed in section 2 in the text.

particles from LEP II. At each mass point, 500k events were produced for pair production of dark pions (all allowable modes). This was done for both $\sqrt{s} = 8$ TeV and $\sqrt{s} = 13$ TeV collisions. The π_D are decayed in the narrow width approximation using `Pythia`.

There is no dedicated search for dark mesons at the LHC. We therefore estimate the existing bounds by recasting a vast set of potentially constraining searches using Monte Carlo methods. We will present our results first, followed by a more detailed description of our recasting methods and a summary of why several searches which look promising at first glance fail to set strong bounds.

3.1 ρ_D constraints

We first consider ρ_D production and decay. The ρ_D dark vector mesons kinetically mix with electroweak gauge bosons, shown in eq. (2.6), giving direct couplings to SM fermions, shown in eq. (2.9). In both the $SU(2)_L$ and $SU(2)_R$ models, there is a neutral ρ_D^0, better known as a new Z' gauge boson. Via kinetic mixing, this ρ_D^0 acquires a coupling to leptons.

The strongest constraints on generic Z' gauge bosons (with masses near or above the electroweak scale) is from the absence of resonances in the the $\ell^+\ell^-$ invariant mass spectrum [130, 131]. Using the ATLAS 13 TeV search with 36.1 fb^{-1} of integrated luminosity [130], we have recast the dilepton searches for the combined electron and muon channels into a limit on ρ_D cross section times branching fraction to leptons. This is accomplished by simulating the production of ρ_D and decaying them according to the branching ratios shown in figure 1. After passing through a parton shower, hadronization, and detector simulation, we select events which contain same-flavor opposite-sign leptons within the ATLAS selection criteria. The combined efficiency (branching ratio times the detector efficiencies) multiplied by the cross section can then be compared against the exclusion limits provided by the ATLAS HEPData [132].

In figure 4, we illustrate the bounds that we have obtained by determining the largest coupling of the ρ_D^0 to the SM for any choice of m_{ρ_D} within the range of interest in this paper. The coupling is completely determined by the model-independent quantity $\epsilon^2 \times BR(\rho_D^0 \rightarrow$
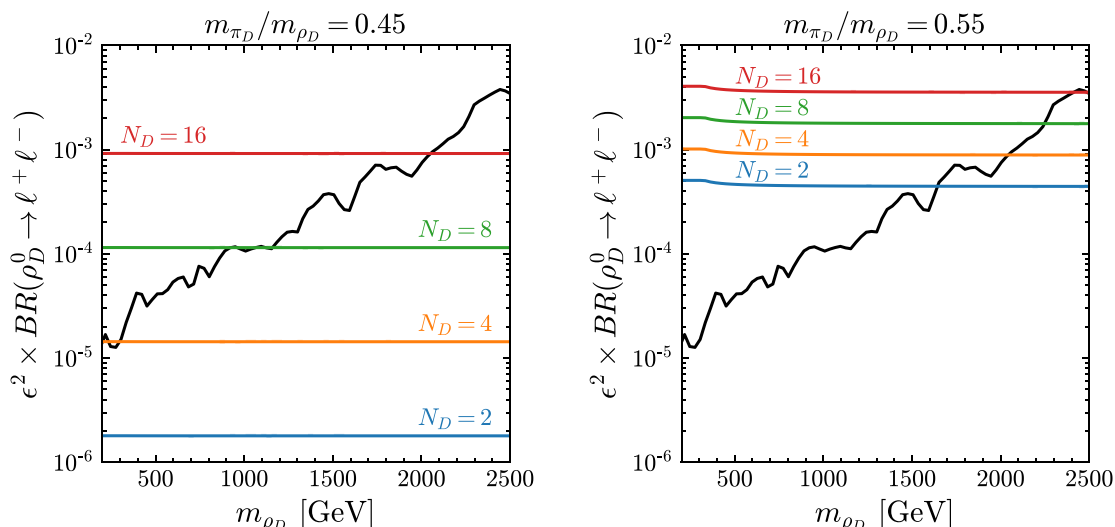
Figure 4. Constraints on the kinetic mixing between the the SM and ρ_D^0 (times the leptonic branching fraction of ρ_D^0) from the non-observation of a dilepton resonance near m_{ρ_D}. The black line is the model-independent limit. To illustrate the impact of this bound on the model space, we have superimposed the predicted $\epsilon^2 \times \mathrm{BR}(\rho_D^0 \to \ell^+\ell^-)$ for the $SU(2)_L$ model, varying the number of colors between 2 to 16. On the right, the 2-body decay $\rho_D^0 \to \pi_d^+\pi_d^-$ is kinematically forbidden, leading to strong constraints: $m_{\rho_D} > 1.5$-$2.5\,\mathrm{TeV}$. On the left, the 2-body decay $\rho_D^0 \to \pi_d^+\pi_d^-$ is open, and we see that when $N_D \lesssim 4$, there is no constraint from resonant ρ_D^0 production and decay to dileptons.

$\ell^+\ell^-$), that is shown as a black line in both panels of figure 4. Also superimposed on the panels are the predicted sizes of $\epsilon^2 \times BR(\rho_D^0 \to \ell^+\ell^-)$ for a given m_{π_D}/m_{ρ_D} and number of dark colors N_D in the $SU(2)_L$ model. It is important to note that ϵ is the kinetic mixing parameter and not the detector efficiency. (Similar but weaker constraints are found in the $SU(2)_R$ model.) The right panel clearly shows that the neutral dark vector meson is strongly constrained by the dilepton data when $m_{\pi_D}/m_{\rho_D} > 0.5$.

The dependence on the number of dark colors is nontrivial:

$$\sigma(pp \to \rho_D^0 \to \ell^+\ell^-) \; \propto \; \epsilon^2 \times BR(\rho_D^0 \to \ell^+\ell^-) \propto \begin{cases} N_D & \eta > 0.5 \\ N_D^3 & \eta < 0.5 \,. \end{cases} \qquad (3.1)$$

In the case $\eta > 0.5$, the one power of N_D comes from ϵ^2 while in the branching fraction the N_D dependence cancels. Contrast this with the case $\eta < 0.5$, where the branching fraction $BR(\rho_D^0 \to \ell^+\ell^-)|_{\eta<0.5} \simeq \Gamma(\rho_D^0 \to \ell^+\ell^-)/\Gamma(\rho_D^0 \to \pi_D\pi_D) \propto N_D^2$. The left panel clearly shows that when $\rho_D \to \pi_D\pi_D$ is both kinematically open ($\eta < 0.5$) and dominates ($N_D \lesssim 4$), there are virtually no LHC constraints on neutral dark vector meson production and decay. (The very narrow region near $m_{\rho_D} \sim 300\,\mathrm{GeV}$ is, as we will see, also constrained by other searches).

The bounds we have obtained from the ATLAS searches for dilepton resonances assumed the width of the new resonance is relatively narrow, $\Gamma(Z')/M_{Z'} \lesssim 0.03$ [130]. In all of the cases with $\eta = 0.55$, where the ρ_D^0 can only two-decay into SM states, the width is

narrow, $\Gamma_{\rm tot}(\rho_D^0)/m_{\rho_D^0} < 10^{-3}$. Once $\rho_D \to \pi_D \pi_D$ is open, we can estimate this partial width [88]

$$\frac{\Gamma(\rho_D \to \pi_D \pi_D)}{m_{\rho_D}} = \frac{\pi}{3N_D}\left(1 - \frac{4m_{\pi_D}^2}{m_{\rho_D}^2}\right)^{3/2} \simeq \frac{4}{N_D} \times \begin{cases} 0.02 & \eta = 0.45 \\ 0.16 & \eta = 0.25 \,, \end{cases} \tag{3.2}$$

where we have evaluated the result for the two values $\eta = 0.45, 0.25$ used in our benchmarks for the paper. Despite the relative strong-coupling among mesons ($g_{\rho_D \pi_D \pi_D} = 4\pi/\sqrt{N_D} \gg 1$), the kinematic suppression of taking $\eta = 0.45$ suppresses the width of the ρ_D^0 to a few percent, and so the ATLAS bounds are fully applicable. For $\eta = 0.25$, the width is now tens of percent that is large enough requiring a re-analysis of the dilepton data to set precise bounds on the ρ_D^0. For $\eta = 0.25, N < 4$, the ρ_D width to mass ratio reaches $\sim$ tens of percent, so a simple recast of the ATLAS bounds is not completely precise. However, given that (i) the bounds on a wide resonance will be weaker than on a narrow resonance, and (ii) the narrow resonance bounds for $N < 4$ are already weak, we conclude that there is no bound on ρ_D^0 for $\eta = 0.25, N < 4$.

There is one additional constraint on the kinetic mixing of ρ_D with SM gauge bosons from LEP constraints on four-fermion effective operators [133]. Integrating out ρ_D^0 results in four-fermion operators of the form

$$\frac{4\pi}{\Lambda^2}\,\bar{e}e\bar{f}f\,, \tag{3.3}$$

where we have used the operator normalization of ref. [133]. Matching the coefficient,

$$\begin{aligned} \frac{4\pi}{\Lambda^2} &= \frac{1}{m_{\rho_D}^2} \times \begin{cases} \epsilon^2 g^2 & \text{SU(2)}_L \text{ model} \\ \epsilon'^2 g'^2 & \text{SU(2)}_R \text{ model} \end{cases} \\ &= \frac{N_D}{16\pi^2 m_{\rho_D}^2} \times \begin{cases} g^4 & \text{SU(2)}_L \text{ model} \\ g'^4 & \text{SU(2)}_R \text{ model} \end{cases}. \end{aligned} \tag{3.4}$$

The strongest constraints from the LEP data suggest $\Lambda \gtrsim 20\,\text{TeV}$ [133]. For the SU(2)$_R$ model, there is no constraint due to the smallness of g'. For the SU(2)$_L$ model, the bound on $m_{\rho_D^0}$ varies from about 250–750 GeV for $N_D = 2$–16. Given the order one uncertainties in the large N_D estimate for the kinetic mixing, this bound is not any stronger than what we have already found from figure 4.

3.2 Constraints on the dark pion coupling to SM

Throughout the paper, we will generally work in the "vector-like" limit (See ref. [114]) where $\frac{m_{SM}}{v_\pi}$ is small and thus single production of π_D is suppressed. This limit is automatically safe from constraints from electroweak precision observables as well as Higgs coupling measurements, and coincides with the demarcation of our model space into the two categories SU(2)$_L$ and SU(2)$_R$. If, however, $\frac{m_{SM}}{v_\pi}$ is not so small, single production of dark pions is possible and relevant to the phenomenology. In the model of bosonic technicolor / induced electroweak symmetry breaking, this sets the strongest constraints [14].
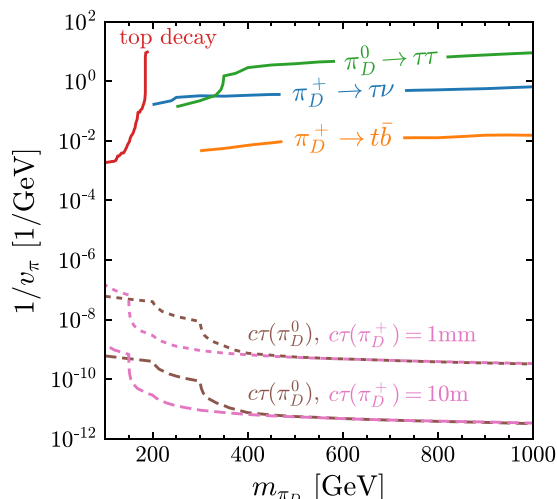
Figure 5. Constraints on the value of $1/v_\pi$ as a function of the dark pion mass. Precise measurements of the top quark exclude regions above the red line. The green, blue, and orange lines come from collider searches for heavy Higgs particles (mainly in 2HDM). Lastly, the brown and pink dashed lines are not constraints, but show at what point the phenomenology changes. Below these lines, the pions start to travel an appreciable distance in the detector, either leading to displaced vertices or disappearing tracks. The lower of these lines are around the scale when the particles leave the detector either as missing energy or look like stable charged particles.

We can also characterize the parameter space of our effective theory by determining the constraints on $1/v_\pi$ of eq. (2.11). In figure 5, we consider several processes[6] where single dark pion production can set upper bounds on $1/v_\pi$. One process is top decay, $t \to \pi_D^+ \bar{b}$. In this process the π_D^+ must be somewhat lighter than the top quark, and thus $\pi_D^+ \to \tau^+ \nu_\tau$ dominates for the charged pions, leading to an excess of τ's in top decay. LHC analyses of top decay, however, are consistent with lepton universality [134, 135]. For values of the pion mass slightly less than the top quark mass, the pion branching ratio to τ is similar to the SM branching ratio of the W to tau. Thus, in this region the branching ratio alone is not enough to constrain the coupling. Instead, we use the total width of the top quark [136–138] as a secondary constraint, and exclude any region where the BSM additions to the top decay change either the width or the tauonic branching ratio by more than two standard deviations away from the measured values. This constraint is shown in red in figure 5.

There are also many searches for the heavy Higgs particles of two-Higgs doublet models that can be recast into searches for single production of the charged or neutral dark pions. In refs. [139, 140], ATLAS searches for a charged Higgs produced association with $t\bar{b}$. The two searches consist of one looking for $H^+ \to \tau^+ \nu_\tau$ while the other looks for $H^+ \to t\bar{b}$. The limits are presented in terms of $\sigma(t\bar{b}H^+) \times BR$, but unfortunately HEPData is not given. We therefore take the limits from plots in refs. [139, 140] and reinterpret them by

---

[6]Note that we only consider processes involving fermions so that we have ξ-independent constraints on $1/v_\pi$. Larger ξ, e.g., $\xi \sim 1$, there can be stronger constraints from couplings to the gauge/Higgs sector [14]. We thank Ennio Salvioni for discussions on this point.

replacing π_D^+ for the charged Higgs boson. The upper bounds on $1/v_\pi$ we obtain are shown in orange and blue in figure 5. Finally, in a similar approach, ref. [141] performed searches for a heavy neutral Higgs boson produced in association with $b\bar{b}$ and decaying to $\tau^+\tau^-$. Upon recasting this search for neutral dark pions, we find somewhat weaker constraints — shown in green in figure 5 — compared with the bounds from charged dark pions.

Finally, while this is not a constraint on the parameter space per se, it is interesting to determine when $1/v_\pi$ is small enough that the decays of the dark pions are no longer prompt in colliders. As a rough guide, we can use

$$\Gamma = \left(\frac{2 \text{ mm}}{c\tau}\right) \times 10^{-13} \text{ GeV} \tag{3.5}$$

and estimate that if $c\tau = 1$ mm, then the neutral pions would lead to displaced tracks, or the charged pions would lead to kinked (or disappearing) tracks when they decay. If $c\tau > 10$ m, then the pions can escape the detectors before decaying, leading to missing energy or long-lived charged tracks. Search strategies for both of these types of signals are interesting but best explored through existing dedicated strategies for long-lived charged or neutral particles [142–145]. The smallness that $1/v_\pi$ needs to be to lead to these long-lived signals is shown in figure 5.

There can also be a contribution to the S parameter as a result of the interactions in eq. (2.11). However, in the ultraviolet strongly-coupled theories considered in ref. [114], we find the contributions depend on the spectrum of the heavier mesons, and so there is no useful translation into bounds on $1/v_\pi$. Suffice to say that there are no bounds from the S parameter when the contributions to the dark fermion masses are mostly vector-like with only smaller contributions arising from electroweak symmetry breaking [6, 146]. In addition, there can also be contributions to the rate for $h \to \gamma\gamma$ with charged dark pions running in the loop. But these contributions are highly suppressed in the same limit that suppresses the S parameter — small contributions to dark fermion masses from electroweak symmetry breaking relative to the vector-like masses.

Clearly, there is a huge range in $1/v_\pi$ — roughly values larger than 10^{-7} and smaller than 10^{-2}, with some slight variation depending on m_{π_D} — where dark pion decays are prompt but the rate for single dark pion production is too small to be detected. Our goal for the remainder of this paper is to explore how prompt LHC searches constrain paired dark pion production in this otherwise open region of parameter space.

4 Resonant dark pion pair-production at LHC

The rate for dark pion pair-production depends on the model — $\text{SU}(2)_L$ versus $\text{SU}(2)_R$, and the NDA estimates for the kinetic mixing as well as the meson self-interactions. It does *not* depend on how the dark pions decay (gaugephilic versus gaugephobic) because the production rate is independent of $1/v_\pi$ and ξ/v_π from eq. (2.11). However, the different decay modes require different search strategies. In table 2, we have denoted different mass regions for each of the categories defined by which decay modes are dominant. The intermediate SM particles, which may subsequently decay, are listed for both the charged

	Mass	Charged Current	Neutral Current
gaugephilic	$m_{\pi_D} \lesssim 150$ GeV	$b\bar{b}\tau\nu$	$\tau^+\tau^-\nu\bar{\nu}$
	150 GeV $\lesssim m_{\pi_D} \lesssim 200$ GeV	$b\bar{b}t\bar{b}$	$t\bar{t}b\bar{b}$
	200 GeV $\lesssim m_{\pi_D} \lesssim 450$ GeV	$Z\,h\,t\bar{b}$	$t\bar{t}b\bar{b}$
	$m_{\pi_D} \gtrsim 450$ GeV	$h\,h\,Z\,W^+$	hhW^+W^-
gaugephobic	$m_{\pi_D} \lesssim 150$ GeV	$b\bar{b}\tau\nu$	$\tau^+\tau^-\nu\bar{\nu}$
	150 GeV $\lesssim m_{\pi_D} \lesssim 220$ GeV	$b\bar{b}t\bar{b}$	$t\bar{t}b\bar{b}$
	220 GeV $\lesssim m_{\pi_D} \lesssim 350$ GeV	$Zht\bar{b}$	$t\bar{t}b\bar{b}$
	$m_{\pi_D} \gtrsim 350$ GeV	$t\bar{t}t\bar{b}$	$t\bar{t}b\bar{b}$

Table 2. Phenomenological regions for collider signatures. The charged and neutral current columns show the SM particles for the dominant branching ratios.

$\left(\pi_D{}^\pm \pi_D{}^0\right)$ and the neutral $\left(\pi_D{}^+ \pi_D{}^-\right)$ currents. Note that the symmetries do not allow for neutral currents of the type $\pi_D{}^0 \pi_D{}^0$, so the SU(2)$_R$ model does not contain a resonantly enhanced charged current.

Table 2 shows that there are many Standard Model particles in the final states, with possibly exotic combinations. We analyzed 13 searches (in addition to the ones already discussed), broken down into 6 searches at 8 TeV and 7 searches at 13 TeV. Surprisingly, we find that many of the searches are not sensitive to our benchmark models. The searches with sensitivity are further detailed here, while we save a discussion of the non sensitive searches for section 4.4.

The results of our recasting are summarized in figure 6. This is the main result of our paper. The top line of each plot (colored in blue) shows the constraints on the model coming from searches for resonant dilepton production. As discussed in the previous section, this depends only on if the ρ_D can decay to leptons or not, and is independent of how the π_D decay. The x axis for the plots is m_{π_D}, so the results are obtained from figure 4 by scaling the x axis by the ratio m_{π_D}/m_{ρ_D}.

The next two lines in the figure 6 display the best constraints we could find for 13 TeV searches. The first of these is a search for supersymmetry in final states with either same-sign leptons or three leptons. Recasted in terms of dark pions, it excludes m_{π_D} in the 200-300 GeV range for the gaugephilic and slightly worse for the gaugephobic categories when $\eta = 0.45$. This search does not work when $\eta = 0.25$ because for fixed m_{π_D}, smaller η implies a heavier ρ and therefore a smaller resonant contribution to pion pair production. The other 13 TeV search with moderate sensitivity is a supersymmetry search with final states of tau leptons. The bounds from this search limit the dark pion mass in all models with $\eta < 0.5$ that we examined to be $\gtrsim 130$ GeV, the mass above which $\pi_D{}^+ \to \tau^+\nu$ ceases to be the dominant decay mode.
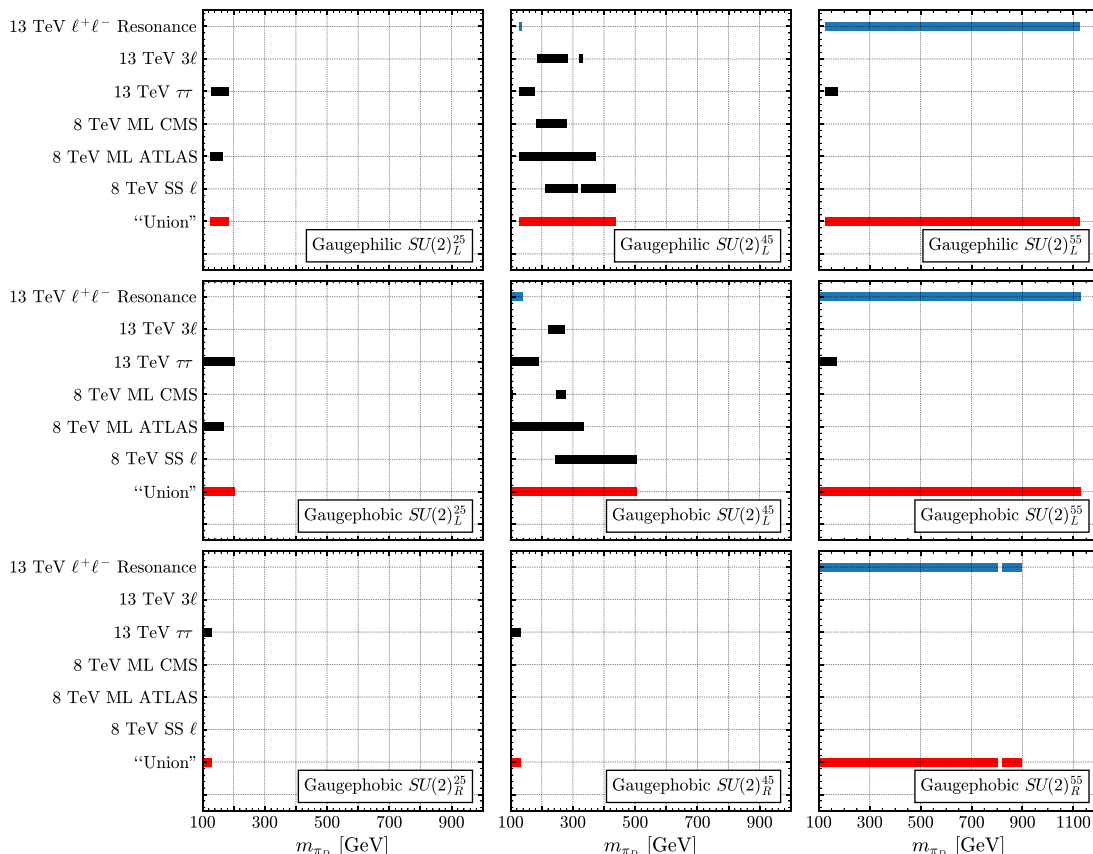
Figure 6. Summary of the dark meson exclusions for the benchmark scenarios and values of the π_D and ρ_D masses. The scenarios are labeled by the type of kinetic mixing, the ratio of the dark pion to dark rho mass $\eta = m_{\pi_D}/m_{\rho_D}$, and the relative strength of the fermionic versus bosonic dark pion decay modes. All of the dark pions decay promptly. The top line indicates the bound on ρ_D^0 inferred from recasting the latest dilepton bounds and interpreted in terms of m_{π_D}. The next five lines (in black) show the π_D mass bound from the most constraining 8 and 13 TeV searches we could find. The union of the exclusions from all of the searches is shown in the last line.

The remaining lines in figure 6 come from the 8 TeV searches which have sensitivity to π_D. Two are multilepton searches from ATLAS and CMS, which are general searches counting the numbers of events for many signal regions. These work well for the models at low masses, and are slightly better for the gaugephilic models. The other exclusion comes from a search for supersymmetry in states with same sign leptons. In particular, one of the signal regions trades the usual missing energy requirement for more b-jets, which works well for the gaugephobic models.

Finally, the last line (shown in red) combines all of the previous constraints in the most naive method. The models where the ρ_D *cannot* decay to π_D are excluded to over $m_{\pi_D} = 1100$ GeV for SU(2) kinetic mixing and to 900 GeV for U(1) (SU(2)$_R$ model). If the mass ratio allows for decays to pions, the exclusion limits are drastically reduced. For $m_{\pi_D}/m_{\rho_D} = 0.45$, the gaugephilic limits are to around 425 GeV while the gaugephobic limits are at 500 GeV for SU(2) mixing. This corresponds to 13 TeV cross sections of 600 fb

and 300 fb, respectively. It is surprising that processes with such distinct final states are still allowed with these large of rates at the LHC. The $SU(2)_R$ model limits are $m_{\pi_D} \gtrsim 130 \, \text{GeV}$, with a cross section of a few pb. As the mass ratio is further extended, the decay products become more energetic, boosting some of the search efficiencies. However, the resulting decrease in the cross section from the heavier ρ_D compensates for this and leads to reduced limits. All of the models with $m_{\pi_D}/m_{\rho_D} = 0.25$ have limits at or below $m_{\pi_D} = 200$ GeV, corresponding to a (13 TeV) cross section of around a pb.

The rates that are still allowed are much larger than one would expect, especially given the exotic combinations of final state particles. In the next subsections, we examine the constraining searches in more detail, looking at why the searches work and what the deficiencies are. The details we expose, combined with the information in section 4.4, will help us identify important elements that future searches should incorporate in order to improve sensitivity to dark pion scenarios.

4.1 Searching for taus

Working from the bottom up of the dark pion mass range, $\mathcal{O}(100\text{–}150$ GeV) dark pions in all of our benchmark models decay primarily as $\pi_D{}^+ \to \tau^+ \nu_\tau$. Therefore, we begin our survey of experimental searches with searches that explicitly look for taus.

ATLAS searches for supersymmetry in electroweak production of supersymmetric particles with final states with τ leptons using 14.8 fb^{-1} of $\sqrt{s} = 13$ TeV data [147]. They interpret the search in terms of the leptons coming from the decays of charginos or neutralinos. As this search is aimed at a supersymmetric model with a neutralino also in the final state, they require a large amount of missing energy, which limits the sensitivity to our benchmarks. The general search strategy is:

1. Trigger on events with two hadronically decaying τs with $p_T > 35(25)$ GeV and have $E_T^{\text{miss}} > 50 \, \text{GeV}$.

2. Require opposite sign taus with $m_{\tau\tau} > 12 \, \text{GeV}$.

3. Veto any event with a b-jet to suppress top-quark backgrounds.

4. Suppress SM backgrounds with a Z boson by removing events with $|m_{\tau\tau} - 79 \, \text{GeV}| < 10 \, \text{GeV}$.[7]

5. Large missing energy cut, $E_T^{\text{miss}} > 150 \, \text{GeV}$.

6. Large *stransverse* mass $m_{T2} > 70 \, \text{GeV}$.

The stransverse mass is defined as

$$m_{T2} = \min_{\mathbf{q_T}} \left[\max \left(m_{T,\tau 1}(\mathbf{p}_{T,\tau 1}, \mathbf{q}_T), m_{T,\tau 2}(\mathbf{p}_{T,\tau 2}, \mathbf{p}_T^{miss} - \mathbf{q}_T) \right) \right], \tag{4.1}$$

where the transverse momenta of the two taus are $\mathbf{p}_{T,\tau 1(2)}$ and $\mathbf{q}_T$ is the transverse vector which minimizes the larger of the two transverse masses. The transverse mass is defined as,

$$m_T(\mathbf{p}_T, \mathbf{q}_T) = \sqrt{2(p_T q_T - \mathbf{p}_T \cdot \mathbf{q}_T)} \,. \tag{4.2}$$
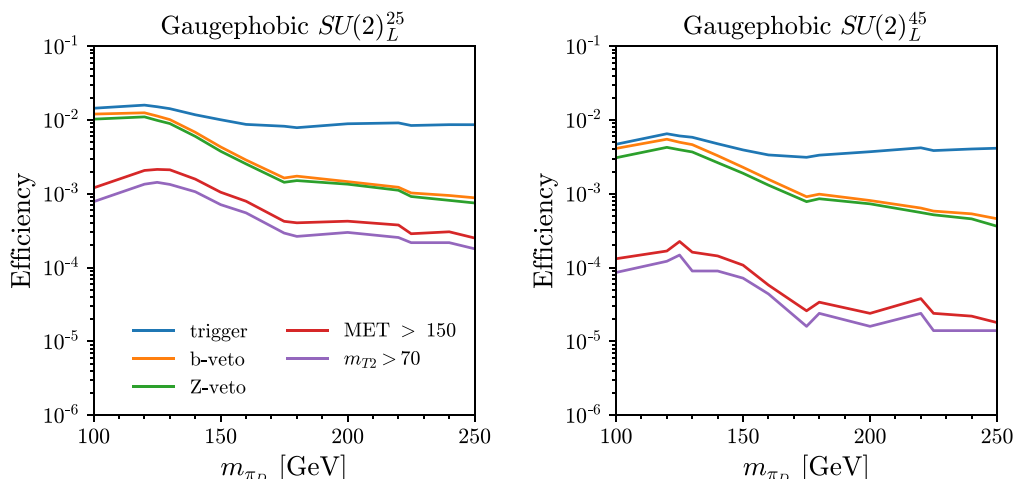
Figure 7. Cut flow for the search for hadronically decaying taus, optimized for electroweak production of supersymmetric particles [147]. The efficiency is much larger for the $\eta = 0.25$ benchmarks than the $\eta = 0.45$ models because the larger ρ_D mass leads to more energetic π_D. This increase in efficiency is offset by the decrease in resonant production cross section.

Figure 7 shows the efficiency of the signal as the various cuts are being made, and exemplifies the kinematic differences between models with different value of η. There is very little loss in efficiency from the b- and Z-vetos for masses less than 150 GeV. Additionally, the figure shows that at this stage, there is very little difference between the η values. However, there is a huge drop in efficiency when requiring large amounts of missing energy. This is not as dramatic in the $\eta = 0.25$ models, which produce more energetic π_D because of the heavier ρ_D.

The exclusions from this search are plotted in figure 8, where the y-axis is the cross section times search efficiency. The expected number of events in the signal region from standard model backgrounds was 5.9 ± 2.1, while only three events were actually observed. As fewer events were seen than expected, the observed limits of 0.32 fb is more stringent than the expected $0.43^{+0.21}_{-0.12}$ fb. Both the gaugephilic and gaugephobic models with SU(2) kinetic mixing and $\eta = 0.25$ or $\eta = 0.45$ are excluded from this search if $m_{\pi_D} \lesssim 170 - 180$ GeV. Surprisingly, this search also constrains the SU(2) models with $\eta = 0.55$ even though the π_D are not produced through a resonant ρ_D. These are only allowed if $m_{\pi_D} > 160$ GeV.[8]

Additionally, the SU(2)$_R$ models [that kinetically mix through U(1)$_Y$] with $\eta = 0.25, 0.45$ are also constrained to be above $m_{\pi_D} \gtrsim 130$ GeV. As shown in the summary plot of figure 6, this is the only search we examined which had sensitivity to the SU(2)$_R^{25,45}$ models.

---

[7]79 GeV is the "visible" mass of the Z for tau decays which have inherent missing energy.

[8]While all of our signal numbers were determined using `Delphes` tagging and identification efficiencies, we derive limits by comparing them with ATLAS/CMS background numbers computed with their own dedicated programs and setting. As the identification and tagging efficiencies in `Delphes` are only an approximation to the true ATLAS/CMS numbers, our signal vs. background comparison is not totally genuine. To quantify the effect of the mismatch, we have checked the ramifications of changing the `Delphes` lepton identification efficiency by $\pm 10\%$ and find that this variation only leads to very minor shifts in the derived m_{π_D} limits.
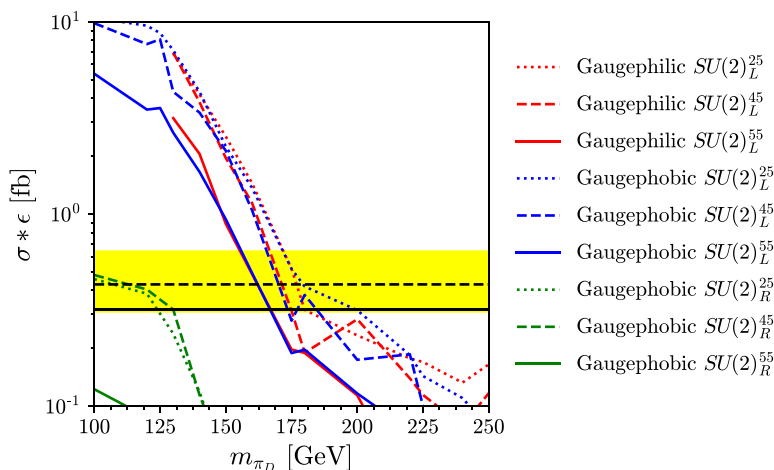
Figure 8. Exclusions from the ATLAS search for supersymmetry in final states with tau leptons [147]. The dark mesons on the lighter side of our spectrum predominately decay to taus, and the cross sections are large. The $SU(2)_L$ type models are excluded if $m_{\pi_D} \lesssim 180$ GeV while the $SU(2)_R$ models limits are around 130 GeV. This is the only search which limits the $SU(2)_R$ models where the ρ_D can decay to $\pi_D\pi_D$.

The reason these limits are not stronger is because the branching ratio to taus is decreasing rapidly as the mass of the pions increases. This is compensated by an increase in the expected number of Ws, Zs, and bs. The next sections examine searches which exploit these particles.

4.2 Generic multilepton searches

Examining table 2, once $m_{\pi_D} \gtrsim 150$ GeV, pair produced dark pions decay to lots of bottom and top quarks, along with Z and W. It should be expected that searches utilizing bs and leptons could place strong constraints on the benchmark models. While we studied many model driven searches and found no limits (see section 4.4), model-independent searches proved useful. Both ATLAS and CMS have a generic search at $8\,\mathrm{TeV}$ based on final states with multiple leptons. (Neither collaboration has repeated the analysis at $13\,\mathrm{TeV}$).

The inclusive ATLAS search looks for 3^+ leptons [148]. The basic search requirements are: 1 electron or muon for triggering purposes ($p_T > 26$ GeV, $|\eta| < 2.5$), a second electron or muon with slightly looser requirements, and a third e/μ or hadronic τ. The events are broken into further sub-categories according to several kinematic variables, such as the b-jet multiplicity, or whether or not the event contains a same-flavor-opposite-sign lepton anti-lepton pair. The signal regions are not orthogonal, and they set bounds on the BSM cross section of roughly a few fb.

Applied to π_D production, we find the most constraining signal regions are those containing a hadronic τ and that contain ≥ 1 b-jet or have low $H_{T,L}$, defined as the scalar sum of the p_T of the three leading leptons (or τ) in the event. The limits depends strongly on the lepton and tau identification. In particular, the ATLAS study used only single-prong
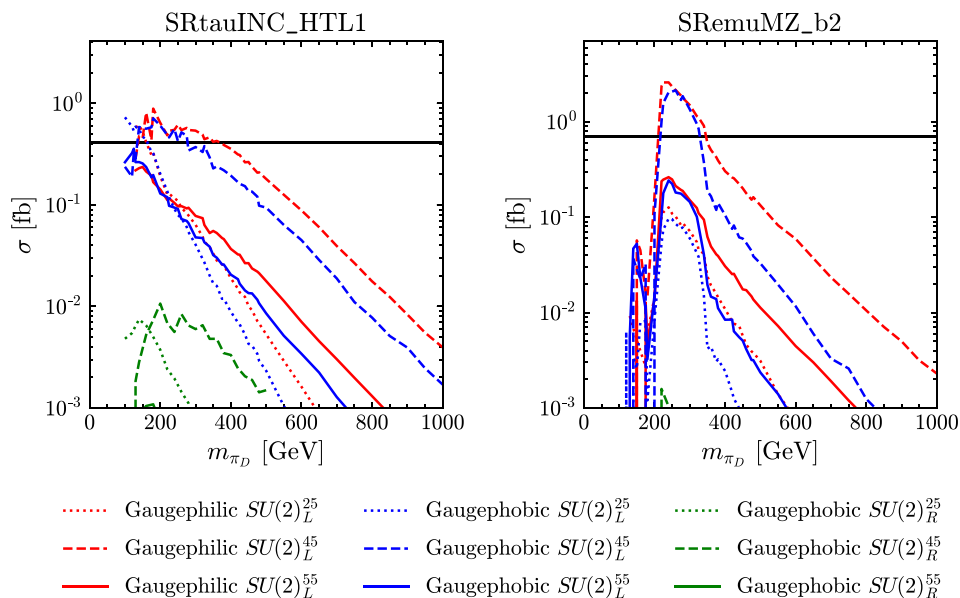
Figure 9. Expected signal cross section in two different signal regions of the ATLAS multilepton search [148] as a function of dark pion mass.

hadronic taus[9] in the analysis and a benchmark identification efficiency of 0.5. Compared to more recent τ reconstruction numbers [149] (which are in the default `Delphes` card), the ATLAS values are worse by a factor of ~ 2. We artificially imposed the reduced tau reconstruction numbers for consistency.

The shape of the exclusion curves for two of the signal regions are shown in figure 9, and exemplify the difference between gaugephilic and gaugephobic models which were not observed in the ditau search discussed in section 4.1. The shapes show that the exclusions closely follow the π_D the branching ratios.

Out of the 144 signal regions defined in the ATLAS search, we find that 16 provide some level of constraint. These are summarized in figure 10. Picking the strongest limit from the signal regions, we find $\pi_D > 370$ GeV in the gaugephilic, $m_{\pi_D}/m_{\rho_D} = 0.45$ case and $\pi_D > 330$ GeV in the gaugephobic, $m_{\pi_D}/m_{\rho_D} = 0.45$ case. For $m_{\pi_D}/m_{\rho_D} = 0.25$ the bounds are looser, due to the fact that smaller m_{π_D}/m_{ρ_D} for fixed m_{π_D} implies a heavier ρ_D, and therefore a smaller resonant contribution to the $pp \to \pi_D\pi_D$ cross section. The difference between the limits in the gaugephilic and gaugephobic can be traced to the presence of more Higgs bosons in the gaugephilic π_D decays, since more Higgs bosons leads to more events with τs or b-jets.

The CMS generic multilepton search is similar, but contains some important differences. It is based on $19.5\,\mathrm{fb}^{-1}$ of $\sqrt{s} = 8\,\mathrm{TeV}$ data [150] and looks for events with either three or four reconstructed leptons. In this case, the definition of leptons includes electrons with $p_T > 10$ GeV and $|\eta| < 2.4$, muons with $p_T > 20$ GeV and $|\eta| < 2.4$, or hadronically decaying taus with $p_T > 20$ GeV and $|\eta| < 2.3$. To trigger, events must contain either

---

[9]Also, there was no dedicated τ trigger in place for this analysis.
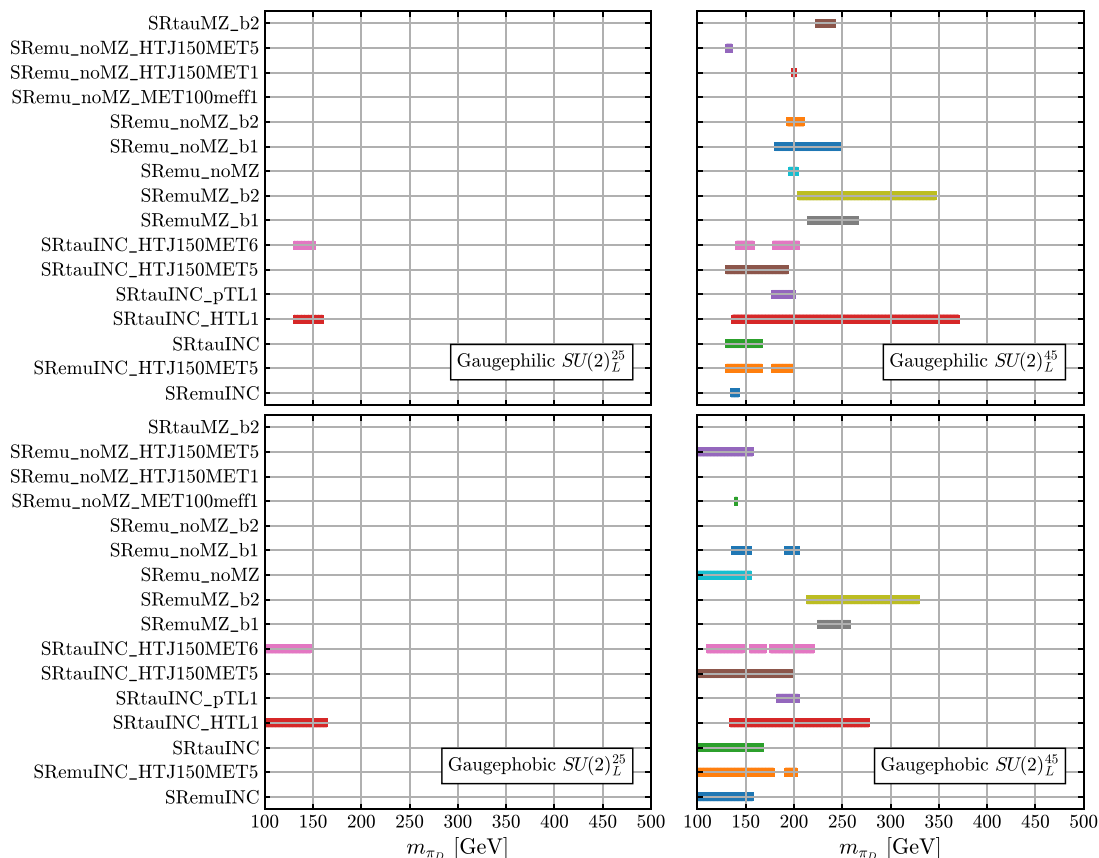
Figure 10. Out of the 144 signal regions defined in ref. [148], 16 regions constrain some portion of the dark meson parameter space. The mass ranges which are colored are excluded. The gaugephilic models have larger branching ratios to Zh and Wh than the gaugephobic models, which leads to greater search efficiency and larger bounds.

an electron or muon with at least $p_T > 20$ GeV and events are only allowed to have one hadronic tau.

The events are divided into 192 independent bins (96 for each of the three or four lepton cases). The bins are split based whether there are same-flavor-opposite-sign (OSSF) pairs of leptons, the invariant mass of existing OSSF pair, the presence of tagged b jets, the number of hadronic τ leptons, the amount of missing energy, and the scalar sum of accepted jet transverse momenta. When CMS combines their signal regions, they are able to set bounds on new physics on the order of $\sigma \times Br \lesssim 100$ fb.

While it would in principle be possible to combine signal regions within our study, CMS does not provide the correlation information. Therefore, we are forced to examine each bin individually. This is in contrast to the method used in the ATLAS search, which used overlapping signal regions, such that some of the regions were more inclusive. Because of this, we find that the exclusions on the benchmarks from the CMS search are not as strong at the ATLAS ones. They are summarized in figure 11 for the signal regions which provide a limit. While the limits are not as strong, we find that the pattern is similar to the ATLAS
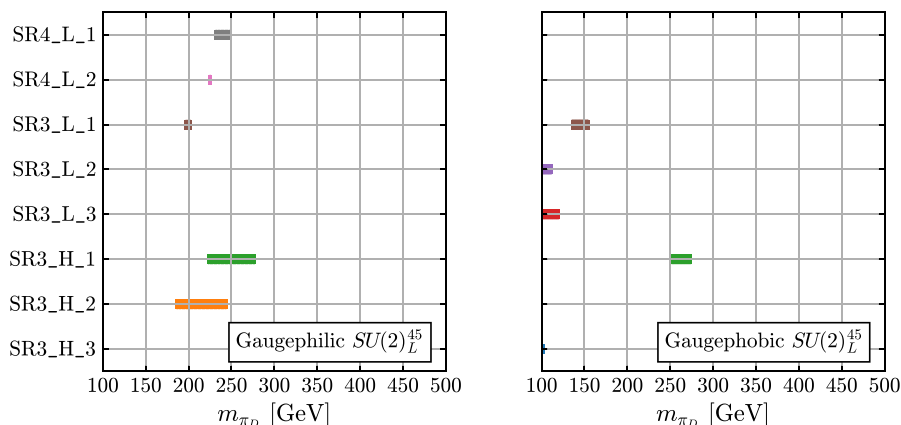
Figure 11. Out of the 192 signal regions defined in the CMS multilepton search [150], 8 regions constrain some part of the dark meson parameter space. The excluded mass ranges are colored according to the denoted signal region. The regions labeled SR3 and SR4 regions contain either 3 or 4 leptons, respectively. The L or H denotes whether the scalar sum of the p_T of the selected jets is less than 200 GeV or greater than 200 GeV. While there are different cuts concerning the number of b-jets or taus, all of the constraining regions require either $E_T^{\rm miss} < 50$ GeV or 50 GeV $< E_T^{\rm miss} \leq 100$ GeV.

result, in that the gaugephilic modes have tighter constraints than the gaugephobic models.

To date, there is no 13 TeV multi-lepton analysis. Given the success we see in the 8 TeV versions at catching models that fall through the cracks in dedicated searches (see section 4.4), we encourage ATLAS and CMS to pursue similar model-independent, inclusive searches in the future.

4.3 Same sign lepton searches

The last type of search that we find has sensitivity to pair produced dark pions is also fairly generic. The main difference is that instead of looking for three or four leptons, they look for multiple leptons of the same electric charge. Frustratingly, the limits we find from these scenarios are stronger from an 8 TeV ATLAS search than the follow-up using a similar analysis strategy at 13 TeV with more integrated luminosity.

The ATLAS search for supersymmetry using 20.7 fb^{-1} of $\sqrt{s} = 8$ TeV collisions in final states with two same sign leptons [151] is a particularly powerful search. The search requires two leptons of the same electric charge. For electrons to be reconstructed, the must have $p_T > 20$ GeV and $|\eta| < 2.47$, while reconstructed muons have $p_T > 20$ GeV and $|\eta| < 2.4$. Jets are reconstructed with the anti-k_t algorithm with a radius parameter of 0.4 and are required to have $p_T > 40$ GeV and $|\eta| < 2.8$. In defining the signal regions, the search makes use of the transverse mass, defined as $m_T = \sqrt{2p_T^\ell E_T^{\rm miss} (1 - \cos \Delta\phi(\ell, E_T^{\rm miss}))}$. In addition, the effective mass is defined as the scalar sum of the transverse momentum of the leading two leptons, the selected jets, and the missing energy.

Three different signal regions are defined. The first signal region has a veto on b-jets, which severely restricts the efficiency for higher mass π_D. For lower masses, there is not
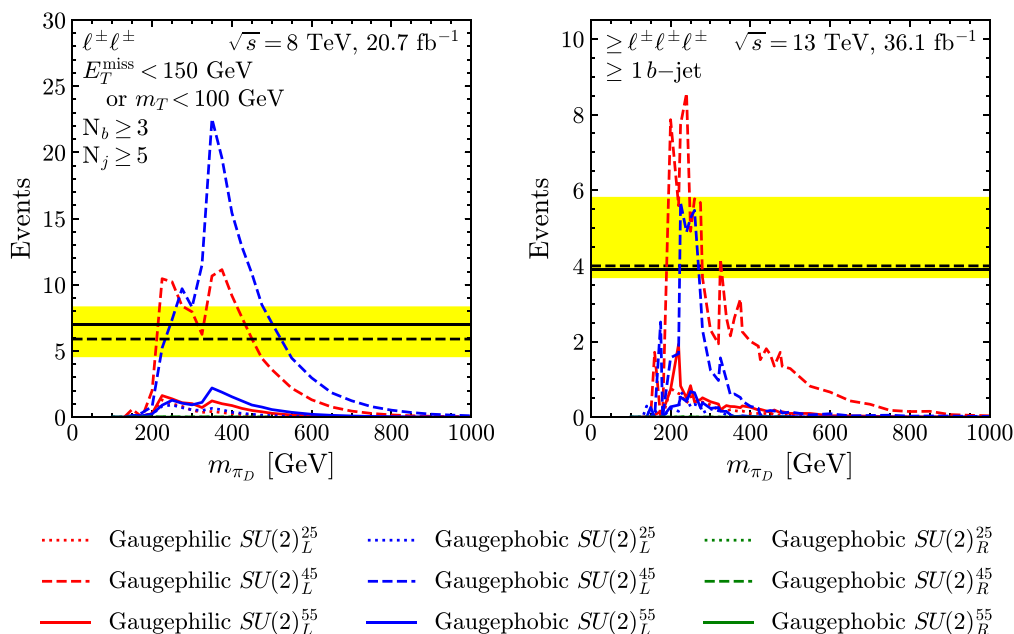
Figure 12. Signal regions of ATLAS searches for three leptons or same sign leptons which have sensitivity to our benchmarks. The left panel shows the limits from the 8 TeV analysis [151] and the right panel has the limits for the 13 TeV analysis [152]. The 8 TeV analysis has bounds to the largest values of m_{π_D} for all of the 8 and 13 TeV analysis which we studied. The 13 TeV search does not do as well because the focus of the analysis shifted to search for higher mass objects.

enough missing energy in the events to pass the cut of $E_T^{\text{miss}} > 150$ GeV, so this signal region does not offer constraints on the model.

The next signal region looks for ≥ 1 b-jet. In addition, there must be at least three jets (can include the b jets), missing transverse momentum > 150 GeV, transverse mass > 100 GeV, and an effective mass > 700 GeV. There are no limits from this region as well, due to the large amount of missing energy required.

The third signal region takes an different approach. In addition to the two same sign leptons, at least three b jets and at least 4 jets overall are required as well. In order to be statistically independent of the other regions, this region looks for events with small amounts of missing energy or transverse mass. The dark pions have no intrinsic missing energy (other than leptonic W decays), but do produce a lot of b quarks, making this an ideal signal region.

In the gaugephilic model, the fraction of decays to $W^{\pm}h$ (Zh) grows with increasing charged (neutral) π_D mass, while dark pions in the gaugephobic case predominantly decays to $t\bar{b}$ ($t\bar{t}$). The difference in branching fractions leads to a smaller average b-jet multiplicity in the gaugephilic case which results in a slightly lower efficiency and, as a consequence, weaker bounds.

To obtain the number of expected signal events, we multiply the cross section and luminosity by the efficiency derived from the analysis cuts. These are then compared to the limits set by ATLAS. In the signal region, 4 events were observed against an expected

background of 3.1 ± 1.6. With this, models which would produce 7.0 expected signal events are excluded at the 95% CL. The left panel of figure 12 shows the results of this signal region with number of expected events for the different models are shown in the red, blue, and green lines. The regions where the expected events extends above the black line are excluded. The only benchmarks which are limited by this search are the $SU(2)_L^{45}$ models. The gaugephilic version is excluded for $210\,\text{GeV} \lesssim m_{\pi_D} \lesssim 420\,\text{GeV}$, while the gaugephobic model is ruled out if m_{π_D} is between $250\,\text{GeV}$ and $500\,\text{GeV}$. These are the strongest limits that we obtained for all of the searches.

With the success of the 8 TeV analysis, there was hope that when the search was extended to 13 TeV, the limits would greatly improve. However, this is not that case. Using $36\,\text{fb}^{-1}$ of $\sqrt{s} = 13$ TeV collisions, ATLAS searched for supersymmetry in final states with two same-sign leptons or three leptons [152]. The basic requirements are nearly the same for the lepton reconstruction, however, the η cut is tightened to $|\eta| < 2.0$ for electrons and loosened to $|\eta| < 2.5$ for muons.

The signal regions are more complicated in the 13 TeV analysis. There are 19 non-exclusive signal regions defined in terms of the number of leptons required; the number of b-jets; the number of jets harder than 25, 40 or 50 GeV, regardless of flavor; the missing energy and effective mass, and the charge of the leptons.

Unlike the previous search at 8 TeV, the 13 TeV search does not have any signal regions which require at least three b-jets. Instead, to cut down on background, the signal regions either require more than 6 jets or large effective mass. This combination is aimed at TeV scale colored particles and does not bode well for searching for pair produced particles with masses in the hundreds of GeV.

The only one of the 19 regions that has sensitivity to heavy dark mesons is the one that does not have requirements on the number of jets, the effective mass, or the missing energy. Instead, it requires at least three leptons of the same-sign and one b-jet. In addition, it requires that no combination of same-sign leptons has an invariant mass around the Z pole (veto $81 < m_{e^\pm e^\pm} < 101$ GeV).

The limits from this region for the different models are shown in the right panel of figure 12. The efficiency is largest in the mass region where $\pi_D^+ \to t\bar{b}$ and $\pi_D^0 \to Zh$ dominate. The $\pi_D^0 \to Zh$ mode is suppressed in the gaugephobic models, hence the limits are not quite as strong as the gaugephilic case. From figure 12, we see that this search only excludes $m_{\pi_D} \sim 200\text{–}400$ GeV for $\eta = 0.45$, while $\eta = 0.25$ models are not constrained at all. Thus, while we expected that updating the best 8 TeV search would yield impressive bounds, it was unable to extend the limits above the $500\,\text{GeV}$ bound set at $\sqrt{s} = 8$ TeV.

This result highlights a troubling trend. We found the strongest limits from the 8 TeV analysis, pushing the mass of the dark pion to $500\,\text{GeV}$ for the most excluded model. However, that search was designed with supersymmetry in mind, and using a supersymmetric interpretation of the 8 TeV search excluded sparticles (stops, specifically) up to 1 TeV. In the supersymmetry interpretation, it makes sense to harden the cuts and focus on particles heavier than 1 TeV. As we have seen in this analysis, however, imposing harder cuts as done with the 13 TeV analyses is detrimental to the signals in our benchmark models, with the result that the older, 8 TeV analyses yielded the strongest constraints. In the next subsection, we discuss other searches which have been thwarted in a similar way.

4.4 Additional searches

According to table 2 (or the branching ratios in figures 2 and 3), we expect pair produced dark pions to result in lots of third generation fermions or gauge/Higgs bosons. However, this is not a unique feature of heavy dark mesons. Many BSM scenarios involve new particles that couple predominantly to gauge/Higgs bosons and third generation fermions, and as a result there are numerous LHC searches (underway, or already done) looking for characteristics signals of, e.g. multiple b-jets, multiple τs, multiple e/μ in association with b-jets or τ, etc. of this type of final states. Based on energy and luminosity alone, the expectation is that one of these 13 TeV searches should be the most constraining. Our results strikingly show this is *not* the case — we find only a few searches constrain dark pions, with the strongest searches coming from 8 TeV.

Our main result, figure 6 came from considering a wide array of BSM searches. While the details of the most successful five searches have been provided in the previous sections, we summarize the other, un-constraining searches in table. 3. In addition to the search channel, we provide a short explanation of why dark pions were so inefficiently captured by the search strategy.

While there are varying reasons the searches in table 3 are not sensitive, there are a few common themes:

1. Searches expect single production. This is especially true for scalars which decay to the Higgs and gauge bosons. To cut down backgrounds, events are vetoed if there are too many objects to be only $V h$.

2. Searches assume large E_T^{miss}. The searches which allow for pair production assume that pair production comes from a sector preserving a Z_2 symmetry and that therefore result in an invisible/dark matter particle at the end of the decay chain. While dark pions in the parameter space we are interested are predominantly pair-produced, they only decay back to SM particles.

3. Searches at 13 TeV have their sights set on heavier new physics. As a result, their cuts are too high to capture lighter dark pions. Heavier dark pions do have higher efficiency, but are not produced at rates the ATLAS and CMS are sensitive to, especially given that there are no leading order QCD-mediated production modes.

4. Data is not presented in a way that is recast-friendly. For instance, the CMS pair produced leptoquark search actually has some minor sensitivity when only using the total number of events. The search then uses the shape of the scalar sum of the p_T of the light lepton, the hadronic τ, and the two jets to set limits, but they do not provide a fit of the shape. Similarly, experiments trying to measure standard model processes (such as $hh \to b\bar{b}\tau^+\tau^-$) may potentially be sensitive to some π_D parameter space, but they rely on machine learning techniques which cannot be reproduced.

We encourage the experiments to continue to push the limits of the LHC searches using all of the techniques they have available. However, as it is not possible for them to test

Search	$\sqrt{s}$ [TeV]	Comments
ATLAS search for a CP-odd Higgs boson decaying to Zh [153]	8	Veto events with more than 2 b-tagged jets kills efficiency
ATLAS search for $t\bar{t}$ resonances [154]	8	Must have exactly one lepton. We have too many jets, confuses search
CMS Pair produced leptoquark [155]	8	Looking for $b\bar{b}\tau^+\tau^-$. Has minor sensitivity to overall rates, would do better with shape analysis but not enough data is provided to recast this.
ATLAS search for SUSY in final states with multiple b-jets [156]	13	Looking for heavy states, so demands large E_T^{miss} and m_{eff}
CMS search for Vh [157]	13	Looking for single production. Needs very boosted hard object.
CMS Di-Higgs $\to \tau\tau\, b\bar{b}$ [158]	13	Neutral pions decay through mixing with the Higgs. Measurement uses BDTs and is not recastable.
CMS Low mass vector resonances $\to q\bar{q}$ [159]	13	Looks for a bump on the falling soft-drop jet mass spectrum. Not enough information to recast the designed decorrelated tagger. Only sensitive to $\sigma \gtrsim 10^3$ pb.
CMS Vector-like $T \to t\, h$ [160]	13	Looking for $t\, h$ resonance, only very heavy and needs QCD production.

Table 3. Possible search strategies which seem like they should set bounds, but have limited-to-no sensitivity.

every theory model, it is important that the results be presented in such a way that they can be reproduced without insider knowledge.

5 Conclusions

- In this paper we have examined the phenomenology of dark pions — composite states with electroweak and Higgs interactions that may lurk at the electroweak scale. Dark pion-like states are a component of many BSM scenarios with new strong dynamics near the electroweak scale.

- In addition to electroweak interactions, dark pions are also resonantly produced via dark rhos that kinetically mix with SM gauge bosons and decay through interactions with SM fermions or into hV. The overall size of the single-pion to SM coupling and the relative strength of the fermionic versus Vh decay modes encodes some information about the symmetry structure of the strong sector and is the subject of ref. [114].

- Taken more abstractly, dark pions represent a type of new physics that is predominantly pair produced, is uncolored, and decays back to SM final states. This is a particularly tricky combination for the LHC, since the lack of strong interactions means the BSM cross sections are small and the fact that the final states are pure SM leaves few easy handles to separate signal from background.

- The phenomenology of the dark pions is governed largely by a few parameters; the relative strength of the dark pion decays to fermionic versus gauge bosons, the type of kinetic mixing [whether with $SU(2)_L$ or $U(1)_Y$], and the mass of π_D relative to ρ_D. Setting up nine benchmark models with different values for these key parameters, we explored the constraints on dark mesons from 8 and 13 TeV LHC searches.

- The only scenario where we find constraints in the TeV range is when the ρ_D^0 is kinematically forbidden from decaying to dark pions and therefore decays with significant branching ratio into leptons, the $SU(2)_{L,R}^{55}$ cases. For all other cases, $\rho_D \to \pi_D \pi_D$ is kinematically accessible so the dilepton bounds are negligible and the best avenue is to look for signals of π_D pairs. Depending on the type of kinetic mixing and the relative mass of the ρ_D mesons, the bounds on m_{π_D} from π_D pair production signals vary from slightly above the LEP II charged particle bound to ~ 500 GeV. The strongest bounds come when the mass of ρ_D is not too much heavier than $2\,m_{\pi_D}$, and kinetically mix with the $SU(2)_L$, while the weakest bounds come when the kinetic mixing only involves $U(1)_Y$. As the most extreme example of how light these particles can be while remaining undetected, consider the $SU(2)_R^{45}$ model. There, dark pions as light as ~ 130 GeV are still viable; perhaps more surprising, the vector ρ_D in this scenario sits at ~ 300 GeV!

- In our survey of LHC searches, we found the most useful features for bounding dark mesons to be signal regions with high multiplicity of leptons and/or b-jets *without* strong requirements on the energy (of the individual objects, or summed) or missing energy. As model-specific searches march towards higher masses in the 13 TeV era, this type of signal region has become rarer and rarer. For scenarios without a dedicated search, such as the dark meson explored here — or, more generally, for types of BSM physics that is pair produced with sub-QCD rates and does not bring a non-SM source of missing energy — the net result is that 13 TeV searches can be less sensitive than 8 TeV versions. Generic searches based on multiple leptons served as a catch-all for this type of "non-standard" BSM at 8 TeV, and we encourage ATLAS and CMS to repeat similar studies with 13 TeV.

Acknowledgments

References

[1] E.H. Simmons, *Phenomenology of a technicolor model with heavy scalar doublet*, *Nucl. Phys.* **B 312** (1989) 253 [INSPIRE].

[2] S. Samuel, *Bosonic technicolor*, *Nucl. Phys.* **B 347** (1990) 625 [INSPIRE].

[3] M. Dine, A. Kagan and S. Samuel, *Naturalness in supersymmetry, or raising the supersymmetry breaking scale*, *Phys. Lett.* **B 243** (1990) 250 [INSPIRE].

[4] A. Kagan and S. Samuel, *The family mass hierarchy problem in bosonic technicolor*, *Phys. Lett.* **B 252** (1990) 605 [INSPIRE].

[5] A. Kagan and S. Samuel, *Renormalization group aspects of bosonic technicolor*, *Phys. Lett.* **B 270** (1991) 37 [INSPIRE].

[6] C.D. Carone and E.H. Simmons, *Oblique corrections in technicolor with a scalar*, *Nucl. Phys.* **B 397** (1993) 591 [hep-ph/9207273] [INSPIRE].

[7] C.D. Carone and H. Georgi, *Technicolor with a massless scalar doublet*, *Phys. Rev.* **D 49** (1994) 1427 [hep-ph/9308205] [INSPIRE].

[8] B.A. Dobrescu and J. Terning, *Negative contributions to S in an effective field theory*, *Phys. Lett.* **B 416** (1998) 129 [hep-ph/9709297] [INSPIRE].

[9] M. Antola, M. Heikinheimo, F. Sannino and K. Tuominen, *Unnatural origin of fermion masses for technicolor*, *JHEP* **03** (2010) 050 [arXiv:0910.3681] [INSPIRE].

[10] A. Azatov, J. Galloway and M.A. Luty, *Superconformal technicolor*, *Phys. Rev. Lett.* **108** (2012) 041802 [arXiv:1106.3346] [INSPIRE].

[11] A. Azatov, J. Galloway and M.A. Luty, *Superconformal technicolor: models and phenomenology*, *Phys. Rev.* **D 85** (2012) 015018 [arXiv:1106.4815] [INSPIRE].

[12] T. Gherghetta and A. Pomarol, *A distorted MSSM Higgs sector from low-scale strong dynamics*, *JHEP* **12** (2011) 069 [arXiv:1107.4697] [INSPIRE].

[13] J. Galloway, M.A. Luty, Y. Tsai and Y. Zhao, *Induced electroweak symmetry breaking and supersymmetric naturalness*, *Phys. Rev.* **D 89** (2014) 075003 [arXiv:1306.6354] [INSPIRE].

[14] S. Chang, J. Galloway, M. Luty, E. Salvioni and Y. Tsai, *Phenomenology of induced electroweak symmetry breaking*, *JHEP* **03** (2015) 017 [arXiv:1411.6023] [INSPIRE].

[15] H. Beauchesne, K. Earl and T. Grégoire, *The spontaneous $\mathbb{Z}_2$ breaking twin Higgs*, *JHEP* **01** (2016) 130 [arXiv:1510.06069] [INSPIRE].

[16] R. Harnik, K. Howe and J. Kearney, *Tadpole-induced electroweak symmetry breaking and PNGB Higgs models*, *JHEP* **03** (2017) 111 [arXiv:1603.03772] [INSPIRE].

[17] T. Alanne, M.T. Frandsen and D. Buarque Franzosi, *Testing a dynamical origin of standard model fermion masses*, *Phys. Rev.* **D 94** (2016) 071703 [arXiv:1607.01440] [INSPIRE].

[18] J. Galloway, A.L. Kagan and A. Martin, *A UV complete partially composite-PNGB Higgs*, *Phys. Rev.* **D 95** (2017) 035038 [`arXiv:1609.05883`] [ɪɴSPIRE].

[19] A. Agugliaro et al., *UV complete composite Higgs models*, *Phys. Rev.* **D 95** (2017) 035019 [`arXiv:1609.07122`] [ɪɴSPIRE].

[20] D. Barducci, S. De Curtis, M. Redi and A. Tesi, *An almost elementary Higgs: theory and practice*, *JHEP* **08** (2018) 017 [`arXiv:1805.12578`] [ɪɴSPIRE].

[21] B. Bellazzini, C. Csáki and J. Serra, *Composite Higgses*, *Eur. Phys. J.* **C 74** (2014) 2766 [`arXiv:1401.2457`] [ɪɴSPIRE].

[22] P.W. Graham, D.E. Kaplan and S. Rajendran, *Cosmological relaxation of the electroweak scale*, *Phys. Rev. Lett.* **115** (2015) 221801 [`arXiv:1504.07551`] [ɪɴSPIRE].

[23] O. Antipin and M. Redi, *The half-composite two Higgs doublet model and the relaxion*, *JHEP* **12** (2015) 031 [`arXiv:1508.01112`] [ɪɴSPIRE].

[24] B. Batell, M.A. Fedderke and L.-T. Wang, *Relaxation of the composite Higgs little hierarchy*, *JHEP* **12** (2017) 139 [`arXiv:1705.09666`] [ɪɴSPIRE].

[25] S. Nussinov, *Technocosmology: could a technibaryon excess provide a 'natural' missing mass candidate?*, *Phys. Lett.* **165B** (1985) 55 [ɪɴSPIRE].

[26] R.S. Chivukula and T.P. Walker, *Technicolor cosmology*, *Nucl. Phys.* **B 329** (1990) 445 [ɪɴSPIRE].

[27] S.M. Barr, R.S. Chivukula and E. Farhi, *Electroweak fermion number violation and the production of stable particles in the early universe*, *Phys. Lett.* **B 241** (1990) 387 [ɪɴSPIRE].

[28] S.M. Barr, *Baryogenesis, sphalerons and the cogeneration of dark matter*, *Phys. Rev.* **D 44** (1991) 3062 [ɪɴSPIRE].

[29] D.B. Kaplan, *A single explanation for both the baryon and dark matter densities*, *Phys. Rev. Lett.* **68** (1992) 741 [ɪɴSPIRE].

[30] R.S. Chivukula, A.G. Cohen, M.E. Luke and M.J. Savage, *A comment on the strong interactions of color-neutral technibaryons*, *Phys. Lett.* **B 298** (1993) 380 [`hep-ph/9210274`] [ɪɴSPIRE].

[31] J. Bagnasco, M. Dine and S.D. Thomas, *Detecting technibaryon dark matter*, *Phys. Lett.* **B 320** (1994) 99 [`hep-ph/9310290`] [ɪɴSPIRE].

[32] M. Yu. Khlopov and C. Kouvaris, *Composite dark matter from a model with composite Higgs boson*, *Phys. Rev.* **D 78** (2008) 065040 [`arXiv:0806.1191`] [ɪɴSPIRE].

[33] T.A. Ryttov and F. Sannino, *Ultra minimal technicolor and its dark matter TIMP*, *Phys. Rev.* **D 78** (2008) 115010 [`arXiv:0809.0713`] [ɪɴSPIRE].

[34] T. Hambye and M.H.G. Tytgat, *Confined hidden vector dark matter*, *Phys. Lett.* **B 683** (2010) 39 [`arXiv:0907.1007`] [ɪɴSPIRE].

[35] Y. Bai and R.J. Hill, *Weakly interacting stable pions*, *Phys. Rev.* **D 82** (2010) 111701 [`arXiv:1005.0008`] [ɪɴSPIRE].

[36] R. Lewis, C. Pica and F. Sannino, *Light asymmetric dark matter on the lattice:* SU(2) *technicolor with two fundamental flavors*, *Phys. Rev.* **D 85** (2012) 014504 [`arXiv:1109.3513`] [ɪɴSPIRE].

[37] M. Frigerio, A. Pomarol, F. Riva and A. Urbano, *Composite scalar dark matter*, *JHEP* **07** (2012) 015 [`arXiv:1204.2808`] [ɪɴSPIRE].

[38] M.R. Buckley and E.T. Neil, *Thermal dark matter from a confining sector*, *Phys. Rev.* **D 87** (2013) 043510 [arXiv:1209.6054] [INSPIRE].

[39] S. Bhattacharya, B. Melić and J. Wudka, *Pionic dark matter*, *JHEP* **02** (2014) 115 [arXiv:1307.2647] [INSPIRE].

[40] D. Marzocca and A. Urbano, *Composite dark matter and LHC interplay*, *JHEP* **07** (2014) 107 [arXiv:1404.7419] [INSPIRE].

[41] A. Hietanen, R. Lewis, C. Pica and F. Sannino, *Fundamental composite higgs dynamics on the lattice:* SU(2) *with two flavors*, *JHEP* **07** (2014) 116 [arXiv:1404.2794] [INSPIRE].

[42] R. Pasechnik, V. Beylin, V. Kuksa and G. Vereshkov, *Composite scalar dark matter from vector-like* SU(2) *confinement*, *Int. J. Mod. Phys.* **A 31** (2016) 1650036 [arXiv:1407.2392] [INSPIRE].

[43] O. Antipin, M. Redi and A. Strumia, *Dynamical generation of the weak and dark matter scales from strong interactions*, *JHEP* **01** (2015) 157 [arXiv:1410.1817] [INSPIRE].

[44] Y. Hochberg et al., *Model for thermal relic dark matter of strongly interacting massive particles*, *Phys. Rev. Lett.* **115** (2015) 021301 [arXiv:1411.3727] [INSPIRE].

[45] A. Carmona and M. Chala, *Composite dark sectors*, *JHEP* **06** (2015) 105 [arXiv:1504.00332] [INSPIRE].

[46] H.M. Lee and M.-S. Seo, *Communication with SIMP dark mesons via Z'-portal*, *Phys. Lett.* **B 748** (2015) 316 [arXiv:1504.00745] [INSPIRE].

[47] Y. Hochberg, E. Kuflik and H. Murayama, *SIMP spectroscopy*, *JHEP* **05** (2016) 090 [arXiv:1512.07917] [INSPIRE].

[48] S. Bruggisser, F. Riva and A. Urbano, *Strongly interacting light dark matter*, *SciPost Phys.* **3** (2017) 017 [arXiv:1607.02474] [INSPIRE].

[49] Y. Wu, T. Ma, B. Zhang and G. Cacciapaglia, *Composite dark matter and Higgs*, *JHEP* **11** (2017) 058 [arXiv:1703.06903] [INSPIRE].

[50] H. Davoudiasl, P.P. Giardino, E.T. Neil and E. Rinaldi, *Unified scenario for composite right-handed neutrinos and dark matter*, *Phys. Rev.* **D 96** (2017) 115003 [arXiv:1709.01082] [INSPIRE].

[51] A. Berlin et al., *Cosmology and accelerator tests of strongly interacting dark matter*, *Phys. Rev.* **D 97** (2018) 055033 [arXiv:1801.05805] [INSPIRE].

[52] S.-M. Choi, H.M. Lee, P. Ko and A. Natale, *Resolving phenomenological problems with strongly-interacting-massive-particle models with dark vector resonances*, *Phys. Rev.* **D 98** (2018) 015034 [arXiv:1801.07726] [INSPIRE].

[53] Y. Hochberg et al., *Strongly interacting massive particles through the axion portal*, *Phys. Rev.* **D 98** (2018) 115031 [arXiv:1806.10139] [INSPIRE].

[54] D.S.M. Alves, S.R. Behbahani, P. Schuster and J.G. Wacker, *Composite inelastic dark matter*, *Phys. Lett.* **B 692** (2010) 323 [arXiv:0903.3945] [INSPIRE].

[55] G.D. Kribs, T.S. Roy, J. Terning and K.M. Zurek, *Quirky composite dark matter*, *Phys. Rev.* **D 81** (2010) 095001 [arXiv:0909.2034] [INSPIRE].

[56] M. Lisanti and J.G. Wacker, *Parity violation in composite inelastic dark matter models*, *Phys. Rev.* **D 82** (2010) 055023 [arXiv:0911.4483] [INSPIRE].

[57] D. Spier Moreira Alves, S.R. Behbahani, P. Schuster and J.G. Wacker, *The cosmology of composite inelastic dark matter*, *JHEP* **06** (2010) 113 [arXiv:1003.4729] [INSPIRE].

[58] M. Geller et al., *Dark quarkonium formation in the early universe*, *JHEP* **06** (2018) 135 [arXiv:1802.07720] [INSPIRE].

[59] S.B. Gudnason, C. Kouvaris and F. Sannino, *Dark matter from new technicolor theories*, *Phys. Rev.* **D 74** (2006) 095008 [hep-ph/0608055] [INSPIRE].

[60] D.D. Dietrich and F. Sannino, *Conformal window of* SU(N) *gauge theories with fermions in higher dimensional representations*, *Phys. Rev.* **D 75** (2007) 085018 [hep-ph/0611341] [INSPIRE].

[61] R. Foadi, M.T. Frandsen and F. Sannino, *Technicolor dark matter*, *Phys. Rev.* **D 80** (2009) 037702 [arXiv:0812.3406] [INSPIRE].

[62] J. Mardon, Y. Nomura and J. Thaler, *Cosmic signals from the hidden sector*, *Phys. Rev.* **D 80** (2009) 035013 [arXiv:0905.3749] [INSPIRE].

[63] F. Sannino, *Conformal dynamics for TeV physics and cosmology*, *Acta Phys. Polon.* **B 40** (2009) 3533 [arXiv:0911.0931] [INSPIRE].

[64] R. Barbieri, S. Rychkov and R. Torre, *Signals of composite electroweak-neutral dark matter: LHC/direct detection interplay*, *Phys. Lett.* **B 688** (2010) 212 [arXiv:1001.3149] [INSPIRE].

[65] A. Belyaev, M.T. Frandsen, S. Sarkar and F. Sannino, *Mixed dark matter from technicolor*, *Phys. Rev.* **D 83** (2011) 015007 [arXiv:1007.4839] [INSPIRE].

[66] LATTICE STRONG DYNAMICS (LSD) collaboration, *Lattice calculation of composite dark matter form factors*, *Phys. Rev.* **D 88** (2013) 014502 [arXiv:1301.1693] [INSPIRE].

[67] A. Hietanen, R. Lewis, C. Pica and F. Sannino, *Composite Goldstone dark matter: experimental predictions from the lattice*, *JHEP* **12** (2014) 130 [arXiv:1308.4130] [INSPIRE].

[68] J.M. Cline, Z. Liu, G. Moore and W. Xue, *Composite strongly interacting dark matter*, *Phys. Rev.* **D 90** (2014) 015023 [arXiv:1312.3325] [INSPIRE].

[69] LATTICE STRONG DYNAMICS (LSD) collaboration, *Composite bosonic baryon dark matter on the lattice:* SU(4) *baryon spectrum and the effective Higgs interaction*, *Phys. Rev.* **D 89** (2014) 094508 [arXiv:1402.6656] [INSPIRE].

[70] G. Krnjaic and K. Sigurdson, *Big Bang darkleosynthesis*, *Phys. Lett.* **B 751** (2015) 464 [arXiv:1406.1171] [INSPIRE].

[71] W. Detmold, M. McCullough and A. Pochinsky, *Dark Nuclei. I: Cosmology and indirect detection*, *Phys. Rev.* **D 90** (2014) 115013 [arXiv:1406.2276] [INSPIRE].

[72] W. Detmold, M. McCullough and A. Pochinsky, *Dark nuclei. II: Nuclear spectroscopy in two-color QCD*, *Phys. Rev.* **D 90** (2014) 114506 [arXiv:1406.4116] [INSPIRE].

[73] J. Brod, J. Drobnak, A.L. Kagan, E. Stamou and J. Zupan, *Stealth QCD-like strong interactions and the* $t\bar{t}$ *asymmetry*, *Phys. Rev.* **D 91** (2015) 095009 [arXiv:1407.8188] [INSPIRE].

[74] M. Asano and R. Kitano, *Partially composite dark matter*, *JHEP* **09** (2014) 171 [arXiv:1406.6374] [INSPIRE].

[75] T. Appelquist et al., *Stealth dark matter: dark scalar baryons through the Higgs portal*, *Phys. Rev.* **D 92** (2015) 075030 [arXiv:1503.04203] [INSPIRE].

[76] T. Appelquist et al., *Detecting stealth dark matter directly through electromagnetic polarizability*, *Phys. Rev. Lett.* **115** (2015) 171803 [arXiv:1503.04205] [INSPIRE].

[77] V. Drach, A. Hietanen, C. Pica, J. Rantaharju and F. Sannino, *Template composite dark matter: SU(2) gauge theory with 2 fundamental flavours*, `PoS(LATTICE 2015)234` [`arXiv:1511.04370`] [INSPIRE].

[78] S. Fichet, *Shining light on polarizable dark particles*, *JHEP* **04** (2017) 088 [`arXiv:1609.01762`] [INSPIRE].

[79] R.T. Co, K. Harigaya and Y. Nomura, *Chiral dark sector*, *Phys. Rev. Lett.* **118** (2017) 101801 [`arXiv:1610.03848`] [INSPIRE].

[80] K.R. Dienes, F. Huang, S. Su and B. Thomas, *Dynamical dark matter from strongly-coupled dark sectors*, *Phys. Rev.* **D 95** (2017) 043526 [`arXiv:1610.04112`] [INSPIRE].

[81] H. Ishida, S. Matsuzaki and Y. Yamaguchi, *Bosonic-seesaw portal dark matter*, *PTEP* **2017** (2017) 103B01 [`arXiv:1610.07137`] [INSPIRE].

[82] A. Francis, R.J. Hudspith, R. Lewis and S. Tulin, *Dark matter from one-flavor* SU(2) *gauge theory*, `PoS(LATTICE 2016)227` [`arXiv:1610.10068`] [INSPIRE].

[83] S.J. Lonsdale, M. Schroor and R.R. Volkas, *Asymmetric dark matter and the hadronic spectra of hidden QCD*, *Phys. Rev.* **D 96** (2017) 055027 [`arXiv:1704.05213`] [INSPIRE].

[84] J.M. Berryman, A. de Gouvêa, K.J. Kelly and Y. Zhang, *Dark matter and neutrino mass from the smallest non-Abelian chiral dark sector*, *Phys. Rev.* **D 96** (2017) 075010 [`arXiv:1706.02722`] [INSPIRE].

[85] A. Mitridate, M. Redi, J. Smirnov and A. Strumia, *Dark matter as a weakly coupled dark baryon*, *JHEP* **10** (2017) 210 [`arXiv:1707.05380`] [INSPIRE].

[86] A. Francis, R.J. Hudspith, R. Lewis and S. Tulin, *Dark matter from strong dynamics: the minimal theory of dark baryons*, *JHEP* **12** (2018) 118 [`arXiv:1809.09117`] [INSPIRE].

[87] G.D. Kribs and E.T. Neil, *Review of strongly-coupled composite dark matter models and lattice simulations*, *Int. J. Mod. Phys.* **A 31** (2016) 1643004 [`arXiv:1604.04627`] [INSPIRE].

[88] C. Kilic, T. Okui and R. Sundrum, *Vectorlike confinement at the LHC*, *JHEP* **02** (2010) 018 [`arXiv:0906.0577`] [INSPIRE].

[89] C. Kilic and T. Okui, *The LHC phenomenology of vectorlike confinement*, *JHEP* **04** (2010) 128 [`arXiv:1001.4526`] [INSPIRE].

[90] R. Harnik, G.D. Kribs and A. Martin, *Quirks at the Tevatron and beyond*, *Phys. Rev.* **D 84** (2011) 035029 [`arXiv:1106.2569`] [INSPIRE].

[91] R. Fok and G.D. Kribs, *Chiral quirkonium decays*, *Phys. Rev.* **D 84** (2011) 035001 [`arXiv:1106.3101`] [INSPIRE].

[92] Y. Bai and P. Schwaller, *Scale of dark QCD*, *Phys. Rev.* **D 89** (2014) 063522 [`arXiv:1306.4676`] [INSPIRE].

[93] Z. Chacko, D. Curtin and C.B. Verhaaren, *A quirky probe of neutral naturalness*, *Phys. Rev.* **D 94** (2016) 011504 [`arXiv:1512.05782`] [INSPIRE].

[94] K. Agashe, P. Du, S. Hong and R. Sundrum, *Flavor universal resonances and warped gravity*, *JHEP* **01** (2017) 016 [`arXiv:1608.00526`] [INSPIRE].

[95] S. Matsuzaki, K. Nishiwaki and R. Watanabe, *Phenomenology of flavorful composite vector bosons in light of B anomalies*, *JHEP* **08** (2017) 145 [`arXiv:1706.01463`] [INSPIRE].

[96] P. Draper, J. Kozaczuk and J.-H. Yu, *Theta in new QCD-like sectors*, *Phys. Rev.* **D 98** (2018) 015028 [`arXiv:1803.00015`] [INSPIRE].

[97] D. Buttazzo, D. Redigolo, F. Sala and A. Tesi, *Fusing vectors into scalars at high energy lepton colliders*, *JHEP* **11** (2018) 144 [arXiv:1807.04743] [ɪɴSPIRE].

[98] P. Schwaller, D. Stolarski and A. Weiler, *Emerging jets*, *JHEP* **05** (2015) 059 [arXiv:1502.05409] [ɪɴSPIRE].

[99] T. Cohen, M. Lisanti and H.K. Lou, *Semivisible jets: dark matter undercover at the LHC*, *Phys. Rev. Lett.* **115** (2015) 171804 [arXiv:1503.00009] [ɪɴSPIRE].

[100] M. Freytsis, S. Knapen, D.J. Robinson and Y. Tsai, *Gamma-rays from dark showers with twin Higgs models*, *JHEP* **05** (2016) 018 [arXiv:1601.07556] [ɪɴSPIRE].

[101] M. Kim, H.-S. Lee, M. Park and M. Zhang, *Examining the origin of dark matter mass at colliders*, *Phys. Rev.* **D 98** (2018) 055027 [arXiv:1612.02850] [ɪɴSPIRE].

[102] T. Cohen, M. Lisanti, H.K. Lou and S. Mishra-Sharma, *LHC searches for dark sector showers*, *JHEP* **11** (2017) 196 [arXiv:1707.05326] [ɪɴSPIRE].

[103] H. Beauchesne, E. Bertuzzo, G. Grilli Di Cortona and Z. Tabrizi, *Collider phenomenology of hidden valley mediators of spin* 0 *or* 1/2 *with semivisible jets*, *JHEP* **08** (2018) 030 [arXiv:1712.07160] [ɪɴSPIRE].

[104] S. Renner and P. Schwaller, *A flavoured dark sector*, *JHEP* **08** (2018) 052 [arXiv:1803.08080] [ɪɴSPIRE].

[105] R. Mahbubani, P. Schwaller and J. Zurita, *Closing the window for compressed Dark Sectors with disappearing charged tracks*, *JHEP* **06** (2017) 119 [*Erratum ibid.* **10** (2017) 061] [arXiv:1703.05327] [ɪɴSPIRE].

[106] O. Buchmueller et al., *Simplified models for displaced dark matter signatures*, *JHEP* **09** (2017) 076 [arXiv:1704.06515] [ɪɴSPIRE].

[107] N. Daci et al., *Simplified SIMPs and the LHC*, *JHEP* **11** (2015) 108 [arXiv:1503.05505] [ɪɴSPIRE].

[108] Y. Hochberg, E. Kuflik and H. Murayama, *Dark spectroscopy at lepton colliders*, *Phys. Rev.* **D 97** (2018) 055030 [arXiv:1706.05008] [ɪɴSPIRE].

[109] T. Han, Z. Si, K.M. Zurek and M.J. Strassler, *Phenomenology of hidden valleys at hadron colliders*, *JHEP* **07** (2008) 008 [arXiv:0712.2041] [ɪɴSPIRE].

[110] J. Kang and M.A. Luty, *Macroscopic strings and 'quirks' at colliders*, *JHEP* **11** (2009) 065 [arXiv:0805.4642] [ɪɴSPIRE].

[111] R. Harnik and T. Wizansky, *Signals of new physics in the underlying event*, *Phys. Rev.* **D 80** (2009) 075015 [arXiv:0810.3948] [ɪɴSPIRE].

[112] S. Knapen, S. Pagan Griso, M. Papucci and D.J. Robinson, *Triggering soft bombs at the LHC*, *JHEP* **08** (2017) 076 [arXiv:1612.00850] [ɪɴSPIRE].

[113] A. Pierce, B. Shakya, Y. Tsai and Y. Zhao, *Searching for confining hidden valleys at LHCb, ATLAS and CMS*, *Phys. Rev.* **D 97** (2018) 095033 [arXiv:1708.05389] [ɪɴSPIRE].

[114] G.D. Kribs, A. Martin and T. Tong, *Effective theories of dark mesons with custodial symmetry*, arXiv:1809.10183 [ɪɴSPIRE].

[115] V. Beylin, M. Bezuglov, V. Kuksa and N. Volchanskiy, *An analysis of a minimal vectorlike extension of the Standard Model*, *Adv. High Energy Phys.* **2017** (2017) 1765340 [arXiv:1611.06006] [ɪɴSPIRE].

[116] G. Ecker, J. Gasser, A. Pich and E. de Rafael, *The role of resonances in chiral perturbation theory*, *Nucl. Phys.* **B 321** (1989) 311 [ɪɴSPIRE].

[117] G. Ecker et al., *Chiral Lagrangians for massive spin 1 fields*, *Phys. Lett.* **B 223** (1989) 425 [INSPIRE].

[118] E. Del Nobile, R. Franceschini, D. Pappadopulo and A. Strumia, *Minimal matter at the Large Hadron Collider*, *Nucl. Phys.* **B 826** (2010) 217 [arXiv:0908.1567] [INSPIRE].

[119] A. Freitas and P. Schwaller, *Multi-photon signals from composite models at LHC*, *JHEP* **01** (2011) 022 [arXiv:1010.2528] [INSPIRE].

[120] Y. Bai and B.A. Dobrescu, *Heavy octets and Tevatron signals with three or four b jets*, *JHEP* **07** (2011) 100 [arXiv:1012.5814] [INSPIRE].

[121] . Alexander et al., *Dark sectors 2016 workshop: community report*, arXiv:1608.08632 [FERMILAB-CONF-16-421].

[122] L. Lee, C. Ohm, A. Soffer and T.-T. Yu, *Collider searches for long-lived particles beyond the standard model*, *Prog. Part. Nucl. Phys.* **106** (2019) 210 [arXiv:1810.12602] [INSPIRE].

[123] J.F. Gunion, H.E. Haber, G.L. Kane and S. Dawson, *The Higgs hunter's guide*, *Front. Phys.* **80** (2000) 1 [INSPIRE].

[124] A. Alloul et al., *FeynRules 2.0 — A complete toolbox for tree-level phenomenology*, *Comput. Phys. Commun.* **185** (2014) 2250 [arXiv:1310.1921] [INSPIRE].

[125] J. Alwall et al., *The automated computation of tree-level and next-to-leading order differential cross sections and their matching to parton shower simulations*, *JHEP* **07** (2014) 079 [arXiv:1405.0301] [INSPIRE].

[126] T. Sjöstrand et al., *An introduction to PYTHIA 8.2*, *Comput. Phys. Commun.* **191** (2015) 159 [arXiv:1410.3012] [INSPIRE].

[127] DELPHES 3 collaboration, *DELPHES 3, a modular framework for fast simulation of a generic collider experiment*, *JHEP* **02** (2014) 057 [arXiv:1307.6346] [INSPIRE].

[128] M. Cacciari, G.P. Salam and G. Soyez, *FastJet user manual*, *Eur. Phys. J.* **C 72** (2012) 1896 [arXiv:1111.6097] [INSPIRE].

[129] M. Cacciari, G.P. Salam and G. Soyez, *The anti-k_t jet clustering algorithm*, *JHEP* **04** (2008) 063 [arXiv:0802.1189] [INSPIRE].

[130] ATLAS collaboration, *Search for new high-mass phenomena in the dilepton final state using $36\,fb^{-1}$ of proton-proton collision data at $\sqrt{s} = 13$ TeV with the ATLAS detector*, *JHEP* **10** (2017) 182 [arXiv:1707.02424] [INSPIRE].

[131] CMS collaboration, *Search for high-mass resonances in dilepton final states in proton-proton collisions at $\sqrt{s} = 13$ TeV*, *JHEP* **06** (2018) 120 [arXiv:1803.06292] [INSPIRE].

[132] ATLAS collaboration, *Search for new high-mass phenomena in the dilepton final state using $36.1\,fb^{-1}$ of proton-proton collision data at $\sqrt{s} = 13$ TeV with the ATLAS detector*, ATLAS-CONF-2017-027 (2017).

[133] ALEPH, DELPHI, L3, OPAL, LEP ELECTROWEAK collaboration, *Electroweak measurements in electron-positron collisions at W-boson-pair energies at LEP*, *Phys. Rept.* **532** (2013) 119 [arXiv:1302.3415] [INSPIRE].

[134] CDF collaboration, *Study of top-quark production and decays involving a τ lepton at CDF and limits on a charged-Higgs boson contribution*, *Phys. Rev.* **D 89** (2014) 091101 [arXiv:1402.6728] [INSPIRE].

[135] ATLAS collaboration, *Measurements of the top quark branching ratios into channels with leptons and quarks with the ATLAS detector*, *Phys. Rev.* **D 92** (2015) 072005 [arXiv:1506.05074] [ɪɴSPIRE].

[136] PARTICLE DATA GROUP collaboration, *Review of particle physics*, *Phys. Rev.* **D 98** (2018) 030001 [ɪɴSPIRE].

[137] D0 collaboration, *An improved determination of the width of the top quark*, *Phys. Rev.* **D 85** (2012) 091104 [arXiv:1201.4156] [ɪɴSPIRE].

[138] CMS collaboration, *Measurement of the ratio* $\mathcal{B}(t \to Wb)/\mathcal{B}(t \to Wq)$ *in pp collisions at* $\sqrt{s} = 8$ *TeV*, *Phys. Lett.* **B 736** (2014) 33 [arXiv:1404.2292] [ɪɴSPIRE].

[139] ATLAS collaboration, *Search for charged Higgs bosons in the* τ+*jets final state using* 14.7 fb^{-1} *of pp collision data recorded at* $\sqrt{s} = 13$ *TeV with the ATLAS experiment*, ATLAS-CONF-2016-088 (2016).

[140] ATLAS collaboration, *Search for charged Higgs bosons in the* $H^{\pm} \to tb$ *decay channel in pp collisions at* $\sqrt{s} = 13$ *TeV using the ATLAS detector*, ATLAS-CONF-2016-089 (2016).

[141] ATLAS collaboration, *Search for additional heavy neutral Higgs and gauge bosons in the ditau final state produced in* 36 fb^{-1} *of pp collisions at* $\sqrt{s} = 13$ *TeV with the ATLAS detector*, *JHEP* **01** (2018) 055 [arXiv:1709.07242] [ɪɴSPIRE].

[142] Z. Liu and B. Tweedie, *The fate of long-lived superparticles with hadronic decays after LHC Run 1*, *JHEP* **06** (2015) 042 [arXiv:1503.05923] [ɪɴSPIRE].

[143] J.A. Evans and J. Shelton, *Long-lived staus and displaced leptons at the LHC*, *JHEP* **04** (2016) 056 [arXiv:1601.01326] [ɪɴSPIRE].

[144] D. Curtin et al., *Long-lived particles at the energy frontier: the MATHUSLA physics case*, arXiv:1806.07396 [ɪɴSPIRE].

[145] J. Liu, Z. Liu and L.-T. Wang, *Enhancing long-lived particles searches at the LHC with precision timing information*, *Phys. Rev. Lett.* **122** (2019) 131801 [arXiv:1805.05957] [ɪɴSPIRE].

[146] R. Barbieri, B. Bellazzini, V.S. Rychkov and A. Varagnolo, *The Higgs boson from an extended symmetry*, *Phys. Rev.* **D 76** (2007) 115008 [arXiv:0706.0432] [ɪɴSPIRE].

[147] ATLAS collaboration, *Search for electroweak production of supersymmetric particles in final states with* τ *leptons in* $\sqrt{s} = 13$ *TeV pp collisions with the ATLAS detector*, ATLAS-CONF-2016-093 (2016).

[148] ATLAS collaboration, *Search for new phenomena in events with three or more charged leptons in pp collisions at* $\sqrt{s} = 8$ *TeV with the ATLAS detector*, *JHEP* **08** (2015) 138 [arXiv:1411.2921] [ɪɴSPIRE].

[149] ATLAS collaboration, *Measurement of the* τ *lepton reconstruction and identification performance in the ATLAS experiment using pp collisions at* $\sqrt{s} = 13$ *TeV*, ATLAS-CONF-2017-029 (2017).

[150] CMS collaboration, *Search for anomalous production of events with three or more leptons in pp collisions at* $\sqrt{s} = 8$ *TeV*, *Phys. Rev.* **D 90** (2014) 032006 [arXiv:1404.5801] [ɪɴSPIRE].

[151] ATLAS collaboration, *Search for strongly produced superpartners in final states with two same sign leptons with the ATLAS detector using* 21 fb^{-1} *of proton-proton collisions at* $\sqrt{s} = 8$ *TeV.*, ATLAS-CONF-2013-007 (2013).

[152] ATLAS collaboration, *Search for supersymmetry in final states with two same-sign or three leptons and jets using 36 fb^{-1} of $\sqrt{s} = 13$ TeV pp collision data with the ATLAS detector*, *JHEP* **09** (2017) 084 [arXiv:1706.03731] [INSPIRE].

[153] ATLAS collaboration, *Search for a CP-odd Higgs boson decaying to Zh in pp collisions at $\sqrt{s} = 8$ TeV with the ATLAS detector*, *Phys. Lett.* **B 744** (2015) 163 [arXiv:1502.04478] [INSPIRE].

[154] ATLAS collaboration, *A search for $t\bar{t}$ resonances using lepton-plus-jets events in proton-proton collisions at $\sqrt{s} = 8$ TeV with the ATLAS detector*, *JHEP* **08** (2015) 148 [arXiv:1505.07018] [INSPIRE].

[155] CMS collaboration, *Search for pair production of third-generation scalar leptoquarks and top squarks in proton–proton collisions at $\sqrt{s} = 8$ TeV*, *Phys. Lett.* **B 739** (2014) 229 [arXiv:1408.0806] [INSPIRE].

[156] ATLAS collaboration, *Search for supersymmetry in final states with missing transverse momentum and multiple b-jets in proton-proton collisions at $\sqrt{s} = 13$ TeV with the ATLAS detector*, *JHEP* **06** (2018) 107 [arXiv:1711.01901] [INSPIRE].

[157] CMS collaboration, *Search for heavy resonances decaying into a vector boson and a Higgs boson in final states with charged leptons, neutrinos and b quarks*, *Phys. Lett.* **B 768** (2017) 137 [arXiv:1610.08066] [INSPIRE].

[158] CMS collaboration, *Search for Higgs boson pair production in events with two bottom quarks and two tau leptons in proton–proton collisions at $\sqrt{s} = 13$ TeV*, *Phys. Lett.* **B 778** (2018) 101 [arXiv:1707.02909] [INSPIRE].

[159] CMS collaboration, *Search for low mass vector resonances decaying into quark-antiquark pairs in proton-proton collisions at $\sqrt{s} = 13$ TeV*, *JHEP* **01** (2018) 097 [arXiv:1710.00159] [INSPIRE].

[160] CMS collaboration, *Search for single production of a heavy vector-like T quark decaying to a Higgs boson and a top quark with a lepton and jets in the final state*, *Phys. Lett.* **B 771** (2017) 80 [arXiv:1612.00999] [INSPIRE].